Flanders
State of
the Art

14_014_6
FHR reports

Methodology for safety assessment 2015

Background report on wave transformation and overtopping calculation by SWASH

DEPARTMENT
**MOBILITY &
PUBLIC
WORKS**

www.flandershydraulicsresearch.be

Methodology for Safety Assessment 2015

Background report on wave transformation and overtopping calculation by SWASH

Suzuki, T.; Altomare, C.; De Roo, S.; Kolokythas, G.; Vanneste, D.; Peeters, P.; Mostaert, F.

Flanders Hydraulics Research
Flanders State of the Art

Cover figure © Eddy Baete

Legal notice

Copyright and citation

This publication should be cited as follows:

Suzuki, T.; Altomare, C.; De Roo, S.; Kolokythas, G.; Vanneste, D.; Peeters, P.; Mostaert, F. (2017). Methodology for Safety Assessment 2015: Background report on wave transformation and overtopping calculation by SWASH. Version 3.0. FHR Reports, 14_014_6. Flanders Hydraulics Research: Antwerp.

Document identification

Customer:	Agentschap Maritieme Dienstverlening en Kust - Afdeling Kust	Ref.:	WL2017R14_014_6
Keywords (3-5):	Wave transformation; overtopping; SWASH		
Text (p.):	60	Appendices (p.):	2
Confidentiality:	☒ Yes	Released as from:	01/01/2020
		Exception:	☒ The Government of Flanders

Author(s):	Suzuki, T.; Altomare, C.; De Roo, S.; Kolokythas, G.

Control

	Name	Signature
Reviser(s):	Vanneste, D.	
Project leader:	Suzuki, T.	

Approval

Coordinator research group:	Peeters, P.	
Head of Division:	Mostaert, F.	

Abstract

A new Safety Assessment methodology has been developed for the ‘Safety Assessment 2015’. One of the key changes compared to the last Safety Assessment methodology for the ‘Safety Assessment 2007’ is the introduction of a numerical model SWASH for wave transformation and wave overtopping calculations. This document is a technical support document (i.e. introduction of SWASH model) showing the necessities and reasons for the changes, the background theories, applicability, validation and new methodologies including some limitations of the model.

Finally, all the detailed methodologies related to wave transformation and wave overtopping using SWASH for the ‘Safety Assessment 2015’ are mainly determined based on this document.

Note that the extra specifications of the SWASH model for the ‘Safety Assessment 2015’ are discussed in WL2017R14_014_7: Updated methodology.

Contents

Abstract III

Contents V

List of tables VII

List of figures VIII

1 Introduction 1

1.1 Background 1

1.2 Outline 1

2 Methodology for 'Safety assessment 2007' 2

2.1 Wave transformation 2

2.2 Wave overtopping 2

3 Numerical models 3

3.1 SWAN model 3

3.2 SWASH model 3

3.3 Mike21-BW 4

3.4 Characteristics of the wave models 4

4 Selection and validation of wave transformation model 5

4.1 Petten sea dike case 5

4.1.1 Field measurements 5

4.1.2 Model settings 6

4.1.3 Applicability of models 11

4.1.4 Computational cost 16

4.1.5 Conclusion 17

4.2 Extra validations for Petten sea dike case 19

4.2.1 Model settings 19

4.2.2 Results 19

4.3 Further validation 2 (case Oostende Noodstrand) 23

4.3.1 Field measurement 23

4.3.2 Model settings 24

4.3.3 Estimation of wave boundary condition at the toe of the dike 24

4.3.4 Computational cost 26

4.4 Conclusion 26

5 Case studies for wave transformation 27

5.1 Wenduine ... 27
5.1.1 Comparison with SWAN for wave transformation ... 27
5.1.2 Directional spreading effect ... 30
5.1.3 Horizontal viscosity effect ... 33
5.2 Special cross sections & Koksijde ... 34
5.2.1 Wave transformation in special cross section ... 34
5.2.2 Wave transformation in Koksijde ... 38
5.3 Conclusion ... 40
6 Validation of wave overtopping calculation by SWASH ... 41
6.1 Petten case ... 41
6.1.1 Settings and validation ... 41
6.1.2 SWASH 1D overtopping calculation result ... 41
6.1.3 EurOtop (2007) overtopping calculation based on SWASH 2D calculation ... 45
6.1.4 Conclusion ... 45
6.2 Wenduine case ... 46
6.2.1 Model settings ... 46
6.2.2 Wave overtopping calculation ... 47
6.2.3 Influence of bottom friction ... 48
6.3 Physical model of Van Doorslaer & De Rouck (2010) ... 50
6.3.1 Physical Model Setup ... 50
6.3.2 Numerical Model Setup ... 50
6.3.3 Wave Propagation ... 51
6.3.4 Mean Wave Overtopping ... 52
6.4 Conclusion ... 54
7 Case study for wave overtopping calculation ... 55
7.1 Wenduine case study ... 55
7.2 Case study - special cross sections & Koksijde ... 56
8 Conclusions ... 57
8.1 Wave transformation ... 57
8.2 Wave overtopping ... 57
8.3 Differences in outcomes from the ‘Safety Assessment 2007’ and ‘2015’ ... 57
9 References ... 59
Appendix A: directional spreading ... A1
Cos model ... A1
Cos2 model ... A1
Comparison of cos model and cos2 model ... A2

List of tables

Table 3-1: Characteristics of each model 4
Table 4-1: The offshore wave condition employed at the wave boundary in the simulation 7
Table 4-2: Wave properties at the toe of the dike 12
Table 4-3: Computational cost for Petten simulations 16
Table 4-4: Computational cost in different boundary conditions in SWASH 2D. 17
Table 4-5: The offshore wave condition employed at the wave boundary in the simulation 19
Table 4-6: Wave properties at the toe of the dike (PT2 case) 20
Table 4-7: Wave properties at the toe of the dike (PT3 case) 21
Table 4-8: Wave properties at the toe of the dike (PT4 case) 22
Table 4-9: Position of measurement buoys 23
Table 4-10: The offshore wave condition employed at the wave boundary in the simulation for Oostende noodstrand case 24
Table 4-11: Computed wave properties at WTR (+1.27 m TAW) by SWASH 25
Table 4-12: Computational cost for Oostende Noodstrand simulations 26
Table 5-1: Wave overtopping estimation in Wenduine. 28
Table 5-2: Hm0, wave set-up and spectral period for different directional spreading (0, 15 and 30 degree) 31
Table 6-1: Wave overtopping discharge in different wave trains (dx = 0.5 m; wave properties are total one, not incident) ~100 waves:20 min 43
Table 6-2: Wave overtopping discharge in each measurement from Petten 44
Table 6-3: Wave overtopping discharge in different wave trains (dx = 0.5 m; wave properties are total one, not incident) 500 waves 44
Table 6-4: Wave overtopping calculation by EurOtop 45
Table 6-5: Wave overtopping calculations (1D): Test Case WEN_004 47
Table 6-6: Overtopping test parameters 51
Table 6-7: Measured incident wave H_{m0} and $T_{m-1,0}$ and mean overtopping discharge ($\overline{q}$) 53
Table 7-1: Wave overtopping estimation in Wenduine 55
Table 7-2: Wave overtopping estimation in special cross section case and Koksijde case 56

List of figures

Figure 4-1: Pictures of measurement points in Petten 6

Figure 4-2. Bathymetry and wave measurement positions. The bathymetrical measurement took place at 15/11/2007, after the storm of 09/11/2007. 6

Figure 4-3: Bathymetry for two-dimensional calculation (left) and the significant wave height distribution (right). 7

Figure 4-4. Comparison of wave spectrum among different grid sizes. 8

Figure 4-5: Above: Petten bathymetry measured on 15/11/2007 and wave measurement positions. Below: Truncated bathymetry at level +1.36 m NAP (only for 1D simulations). 10

Figure 4-6: Spatial distribution of total significant wave height (SWAN* & SWASH) 12

Figure 4-7: Wave-energy spectra computed by SWASH (1D & 2D) and SWAN at the wave-gauge positions (from 031 to 071) compared to corresponding field measurements. 13

Figure 4-8: Wave-energy spectra computed by MIKE 21 BW (1D) and SWASH (1D & 2D) at the wave-gauge positions (from 031 to 071) compared to corresponding field measurements. 14

Figure 4-9: Wave-energy spectra computed by MIKE 21 BW (2D) and SWASH (1D & 2D) at the wave-gauge positions (from 031 to 071) compared to corresponding field measurements. 15

Figure 4-10: Comparison of wave energy spectrum (default boundary vs periodic boundary) 17

Figure 4-11. Topography and wave measurement positions. The bathymetry measurement was in November 2011 19

Figure 4-12: Wave-energy spectra computed by SWASH 2D compared to corresponding field measurements (PT2 case) 20

Figure 4-13: Wave-energy spectra computed by SWASH 2D compared to corresponding field measurements (PT3 case) 21

Figure 4-14: Wave-energy spectra computed by SWASH 2D compared to corresponding field measurements (PT4 case) 22

Figure 4-15: Geometry for the wave calculation* 23

Figure 4-16: Time series of Hs boei, Hs WTR, Tm-1,0 WTR and tij. 24

Figure 4-17: Wave spectrum at WTR (+1.27 m TAW) 25

Figure 5-1: Wave height distribution (Green line: SWAN, Blue circle: SWASH 2D) without dike (incident wave information is obtained). 28

Figure 5-2: Wave spectrum (Green line: SWAN, Blue circle: SWASH 2D) without dike (incident wave information is obtained). WG position is from offshore to the toe 29

Figure 5-3: Spatial distribution of Hm0, wave set-up and spectral period for different directional spreading (0, 15 and 30 degree) 31

Figure 5-4: Wave spectrum for different directional spreading (0, 15 and 30 degree) 32

Figure 5-5: Wave spectrum with and without horizontal viscosity 33

Figure 5-6: Special cross sections tested in SWASH 2D. 34

Figure 5-7: Wave energy spectrum calculated in SWASH 2D (small sand berm case). 35

Figure 5-8: Wave energy spectrum calculated in SWASH 2D (long and short berm case). 35

Figure 5-9: Wave properties calculated in SWASH 2D (small sand berm case). 36

Figure 5-10: Wave properties calculated in SWASH 2D (long and short berm case). 37

Figure 5-11: Wave energy spectrum calculated in SWASH 2D (Koksijde case). 38

Figure 5-12: Wave properties calculated in SWASH 2D (Koksijde case). 39

Figure 6-1: Calibrated the wave spectrum (blue line) at the toe of the dike. 42

Figure 6-2: Overtopping volume per times (individual overtopping) at 3:20 on 9/11/2007, 25 times. 43

Figure 6-3: Wenduine physical model 46

Figure 6-4: SWASH 1D overtopping calculation using n=0.000 and n=0.012 48

Figure 6-5: Physical and numerical model domains (prototype scale) for Case 2 50

Figure 6-6: Energy density spectra computed with the numerical model (black line) and the JONSWAP spectrum with H_{m0} = 2.5; T_p = 12 s and γ = 3.3 (red line) at different stations for test case GEN_001 51

Figure 6-7: (a) Significant wave height, H_{m0} (b) wave period, $T_{m-1,0}$ (c) wave setup and (d) wave period, T_p computed by numerical model for test case GEN_001 52

Figure 6-8: Non-dimensional computed (crosses) mean wave overtopping discharge plotted against EurOtop (2007) equation (thick line) for shallow foreshores 53

1 Introduction

1.1 Background

A new Safety Assessment methodology has been developed for the 'Safety Assessment 2015' and summarized in Suzuki *et al.* (2016). One of the key changes compared to the last Safety Assessment methodology (IMDC, 2008) for the 'Safety Assessment 2007' is the introduction of a numerical model SWASH (Zijlema *et al.*, 2011) for wave transformation and wave overtopping calculations. This document is a technical support document (i.e. introduction of SWASH model) showing the necessities and reasons for the changes, the background theories, applicability, validation and new methodologies including some limitations of the model.

1.2 Outline

First, the methodology of the 'Safety Assessment 2007' (IMDC, 2008) is introduced in Chapter 2 focusing on the model for wave transformation and wave overtopping used in the 'Safety Assessment 2007'.

Second, a quick review of numerical models follows in Chapter 3. It provides an overview of possible numerical wave models to be applied to the 'Safety Assessment 2015', both from theoretical (e.g. basic equations) and practical (e.g. computational cost) point of view.

After the quick review, a comparison of the numerical wave models against in-situ measurements near Petten dike, The Netherlands which has similar configuration with Belgian coastal dikes is conducted in Chapter 4. The aim of the comparison is to figure out which model is the most suitable as a wave transformation model for the 'Safety Assessment 2015', taking into account both accuracy and feasibility (e.g. computational cost). The SWASH model is chosen as the wave transformation model for the 'Safety Assessment 2015' based on the investigations above. After the selection of the model, further validations for wave transformation are conducted using additional field measurement data obtained at Petten and Oostende Noodstrand. In Chapter 5, some particular case studies for wave transformation (Wenduine, special cross sections and Koksijde cases) are performed.

The SWASH model validation for wave overtopping is conducted in Chapter 6, again using first field measurement data of the Petten dike case. After that, physical models cases in Wenduine and UGent (Van Doorslaer & De Rouck, 2010) are used for the final validation. Chapter 7 contains case studies (Wenduine, special cross sections and Koksijde cases) for wave overtopping.

Finally, the conclusions of this report are summarized in Chapter 8.

2 Methodology for 'Safety assessment 2007'

2.1 Wave transformation

In the last Safety Assessment methodology defined in 2007 (IMDC, 2008), the estimation of wave boundary condition at toe of dike in the shallow foreshore is based on SWAN model (Booij *et al.*, 1999), a commonly used spectral domain wave model for coastal engineering. The model has been validated based on Petten data (Delft Hydraulics and Alkyon, 2003) and field measurement data obtained on the the "Noodstrand" in Oostende.

The SWAN 1D model results at the 5 Hs location (5 times significant wave height distance from the geometrical toe of the dike, namely 25 m: the position of toe of dike was defined at the points where the dike slope meets the foreshore) are used for the wave overtopping calculation and the stability calculation of the dike.

The detailed SWAN settings used in the 'Safety Assessment 2007' are shown below.

- Grid resolution 1 m
- Frequency domain 0.04 Hz to 1 Hz with 34 components
- Directional spreading as $\cos^2$ function : 30 degree
- 3rd-generation mode KOMEN
- White-capping OFF
- Triads ON
- Breaking index 0.73
- FRICTION JONSWAP coefficient 0.067m^2s^{-3}
- Wave setup ON

The improvements that have been adopted with respect to the default settings are shown below.

- Actual measured spectra as a precondition
- Triads ON
- Number of iterations increase to 100

The boundary conditions are shown below.

- Water level: the relevant one corresponding to the return period
- Spectrum of a run from the NNW (the wave height of the -5 m contour line is used to scale the spectrum)
- Wind speed and direction: 30 m/s and perpendicular to the coast.

2.2 Wave overtopping

In the last Safety Assessment methodology defined in 2007 (IMDC, 2008), the estimation of mean wave overtopping was based on semi-empirical formulae (see §8.5 of IMDC, 2008). Mostly the formulae were referring to TAW (TAW, 2002) for dikes and Den Heijer (1998) for quay walls. It has to be noticed that the formulae from TAW (2002) are formally the same ones reported afterwards into the European Overtopping Manual, EurOtop (Pullen *et al.*, 2007).

3 Numerical models

Flanders Hydraulics Research is using several numerical wave models for studying the coastal research/management/practice applied to the Belgian coast. These models have the potential to be used as a wave transformation model in the 'Safety Assessment 2015'. In this chapter, each model with the potential to be employed in the 'Safety Assessment 2015' is briefly described.

3.1 SWAN model

SWAN (Booij *et al.*, 1999) is an open source spectral domain wave model used in the methodology in the last 'Safety Assessment 2007'.

Strong points of the SWAN model are that 1) the calculation time is short and 2) the wave transformation is well validated in the near-shore area. On the other hand, a weak point of SWAN is that it cannot deal with infra-gravity waves in the shallow-water zone since according to the wave theory, free long waves will appear due to the release of bounded waves by wave breaking in the shallow-water zone. Those positive and negative characteristics are originated by the fact that the SWAN model is a spectral wave model, and not a time-domain wave model.

It is stated in the last methodology book (IMDC, 2008) that the SWAN model is validated by Petten data (Delft Hydraulics and Alkyon, 2003) and measurement data on the Noodstrand in Oostende, however the data in shallow zone was not processed. Long waves were not included in the wave analysis in Petten: waves were analyzed with a cut off frequency of 0.03 Hz (about T=30 s) to remove the influence of tide. Long wave data in the measurement data Noodstrand, Oostende was not used since the energy in the low frequencies was estimated as spurious. Therefore, the validation cases in the last Safety Assessment are no longer considered to be fully valid for the 'Safety Assessment 2015'.

3.2 SWASH model

SWASH (Zijlema *et al.*, 2011) is an open source time domain wave model. The SWASH model has been used by Flanders Hydraulics Research since it has been officially released in 2011.

Strong points of the SWASH model are that 1) calculation of infra-gravity waves is possible: free long waves are generated in shallow zone and 2) wave transformation is well validated even in the shallow zone (e.g. Suzuki *et al.*, 2011). On the other hand weak point of the SWASH model is that the computational cost is relatively expensive compared to SWAN. Those positive and negative characteristics are due to the fact that the SWASH model is a time domain wave model.

SWASH can be also used for the wave overtopping calculations for shallow foreshore (e.g. Suzuki *et al.*, 2011; Suzuki *et al.*, 2012; Suzuki *et al.*, 2014) and a vertical quay wall (Vanneste *et al.*, 2014). Note that there are some limitations for some configurations e.g. a storm wall on a quay wall (Vanneste *et al.*, 2014) and Stilling Wave Basin concept (Van Doorslaer *et al.*, 2015).

3.3 Mike21-BW

Mike21-BW (BW after Boussinesq-Wave, developed at DHI) (Danish Hydraulic Institute, 2015) is a commercial time-domain wave model. The model is mainly used for the calculation of wave penetration into harbors (Gruwez et al., 2011 and 2012). The governing equation of the model is the Boussinesq equation. The model has been used at Flanders Hydraulics Research since 2010 (e.g. Gruwez *et al.*, 2012). It is a candidate for the new methodology for the 'Safety Assessment 2015'.

The main argument in favor of Mike21-BW is that it has been validated and applied to several case studies of Belgian harbors, including Oostende, Zeebrugge and Blankenberge (e.g. Suzuki *et al.*, 2012). On the other hand, Mike21-BW: (i) has not been used for the wave transformation in the shallow foreshore, and (ii) the computational cost is as expensive as for the SWASH model.

3.4 Characteristics of the wave models

The characteristics of each wave transformation model are summarized in Table 3-1.

Table 3-1: Characteristics of each model

Model name	**Governing equation**	**Model type**	**Computational cost***
SWASH 1D	NLSW equation	Time domain	Not expensive, O(10 min)
SWASH 2D	NLSW equation	Time domain	Expensive, O(1 h)
SWAN 1D	Wave action eq.	Spectral domain	Fast, O(1 min)
Mike21BW 1D	Boussinesq equation	Time domain	Not expensive, O(10 min)
Mike21BW 2D	Boussinesq equation	Time domain	Expensive, O(1 h)

*The computational cost is an estimation based on the computational process.

4 Selection and validation of wave transformation model

4.1 Petten sea dike case

In this section, all the wave models listed in Chapter 3 are validated by means of field measurement data obtained at the Petten sea dike in the Netherlands. After the exploratory comparison, one model is chosen for extra validation, sensitivity analysis and case studies.

4.1.1 Field measurements

In this study, in-situ measurement data set from Petten sea dike in the Netherlands is used to validate wave transformation. Rijkswaterstaat had conducted field measurements at the Petten site in the Netherlands for 20 years since 1994 (Wenneker *et al.*, 2016). Data such as still water level, wind, wave propagation, wave run-up and wave overtopping discharge were obtained. Note that wave overtopping was measured only since 2006. Wave overtopping events were observed several times, and one of which was on 9th November 2007. The data set obtained at 3:20 a.m. on that day has been applied to this study.

The wave directional spreading and wave direction are measured by directional wave buoys 011 and 021, both located 8 km and 3 km offshore respectively from 031. The water surface time series is measured by wave directional buoys 011, 021, and also by wave buoys 031, 161, 171, 181, 061 and 071, see Figure 4-1.

The sampling frequency of the wave buoy data is 4.00 Hz at buoys 031, 161, 171, 181, 061 and 071, and 2.56 Hz at the directional wave buoys 011, 021 and 031. Wave overtopping s recorded when a wave overtopping by one wave occurs at the wave overtopping tank placed on the middle of the dike (at +6.70 m NAP). The beginning and the ending time of an individual wave overtopping volume are available. Therefore it is possible not only to calculate the number of the wave overtopping events in the unit time duration but also the average wave overtopping rate in one wave. The post-processing for the wave parameters and the wave spectrum is based on time series with a duration of 20 minutes. However the raw data were re-analyzed by FHR in this study in order to obtain detailed information on the low-frequency spectral component, since the low frequency wave data were originally cut off at 0.03 Hz during the post-processing, leading to the omission of the low frequency component in the processed dataset.

The bathymetry just after the storm of 9th November 2007 (dated on 15th November 2007) is also available. Figure 4-2 shows the bathymetry data in the cross section of the wave buoys from 071 to 031, which direction is almost perpendicular to the dike and between WNW to NW. The dike crest level in the figure was set at +6.70 m NAP, which is the top level of the wave overtopping box and the configuration of the dike behind the wave overtopping box is not representing the local geometry since this part is optimized for the model runs. A uniform cross-shore bathymetry is applied to the along-shore direction for the sake of simplicity.

Figure 4-1: Pictures of measurement points in Petten

Figure 4-2. Bathymetry and wave measurement positions. The bathymetrical measurement took place at 15/11/2007, after the storm of 09/11/2007.

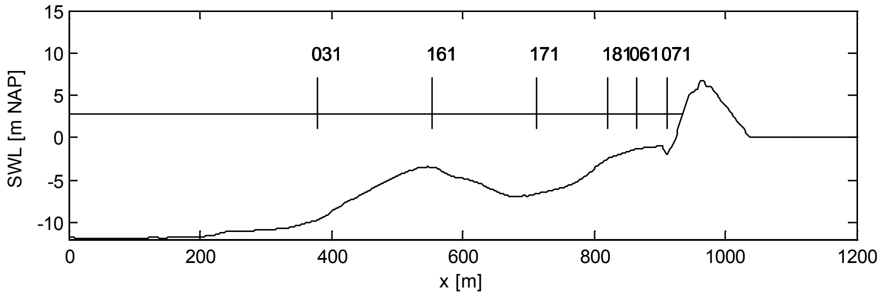

4.1.2 Model settings

SWASH model setup

A two-dimensional wave transformation calculation is conducted by SWASH (version 2.00). One layer is used in the vertical direction since the *kd* value (k is the wave number, and d is the depth) at the wave boundary in the target model condition is 0.5 which gives 1% error in terms of phase velocity (The SWASH team, 2016). Thus it is assumed that the one layer model still resolves the frequency dispersion to an acceptable degree of accuracy.

The wave boundary conditions used in the model runs are shown in Table 4-1. The wave height H_{m0} is 4.6 m which is close to the value observed at the deep water wave buoy 031 while the peak wave period T_p is set as 11.0 s taking into account the offshore buoy spectral period $T_{m-1,0}$ which is 9.56 s at location 021, assuming a constant wave period from offshore in deep water. A JONSWAP spectrum with γ=2.5 is used to be able to get similar offshore wave spectrum shape in the calculations. The wave direction at 3:20 is NW, which is almost perpendicular direction to the dike. Therefore the wave main direction is set at 0 degree, i.e. perpendicular to the dike. The directional spreading (DSPR; see Appendix A) is set to 22.4 degrees taking into account the directional spreading data measured at locations 011 and 021. From a geometrical point of view, directional spreading data at 021 would be the most appropriate for the wave boundary in the domain defined in this study, however the directional spreading data is missing at 021 at 3:20. Therefore, data at 011 at 3:20 is used to obtain the directional spreading by using the relationship between 011 and 021. Concretely, the directional spreading at 3:20 at 011 is 27 degrees and the difference in average directional spreading between 011 and 021 is 4.6 degrees in a wave dataset between 8th to 9th November 2007.

The wave generation is based on the second-order wave theory so that the spurious long waves can be eliminated (e.g. Ottesen Hansen *et al.*, 1979; Barthel *et al.*, 1983). A weakly reflective boundary condition (this means that target waves are generated at this boundary however reflected waves from onshore are radiated) is applied at the wave boundary, and the Sommerfeld radiation condition is applied at the end of the numerical domain, in order to minimize the effect of the reflection. A Manning *n* value of 0.019 was used as a bottom friction.

The initial time step is set to 0.01 s. Note that the calculation time step is automatically adjusted in the calculation depending on the CFL condition. In this study a maximum CFL value of 0.5 is used. In the numerical settings, the non-hydrostatic pressure term in the momentum equations is activated. As indicated in Suzuki *et al.* (2011), the non-hydrostatic pressure plays an important role in the wave propagation. The Keller box scheme is applied since it is one layer calculation.

The time duration of the numerical simulations is 20 minutes, the same duration as in the post-processing of the in-situ measurement.

Table 4-1: The offshore wave condition employed at the wave boundary in the simulation

Date	Time	SWL	H_{m0}	T_p	Dir spr.	Direction
[-]	[-]	[m NAP]	[m]	[s]	[deg]	[deg]
09/11/2007	3:20	2.82	4.6	11.0	22.4	0.0

The two-dimensional calculation domain is shown in the left figure in Figure 4-3. The unit of the level is m NAP. The domain size is 1200 m in x-direction and 1600 m in y-direction. The domain size of y-direction is set long enough not to be influenced by the side boundary of the model. Since the boundary condition at the side walls are set as closed boundaries, the waves are reflected at the side boundary. Even though the wave height distribution is almost uniform in y-direction as shown in the right figure in Figure 4-3, which indicates the wave field is successfully obtained in the cross sections in the middle of the domain. In section 4.1.4, we also tested periodic boundary condition.

Figure 4-3: Bathymetry for two-dimensional calculation (left) and the significant wave height distribution (right).

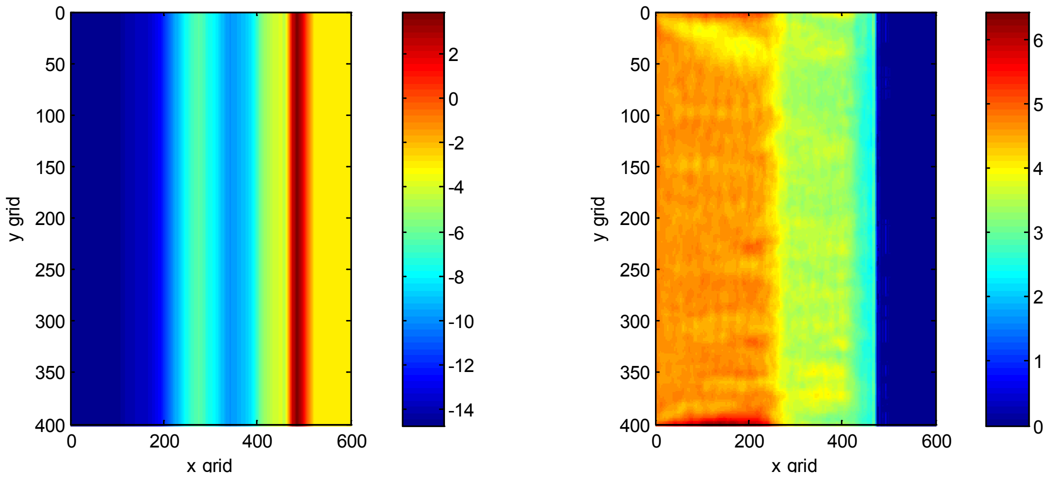

The grid size in x-direction (i.e. cross-shore direction) is determined by a sensitivity analysis in a one-dimensional calculation. Only the grid size in cross-shore direction is investigated since the grid size is important for the wave propagation, wave run-up and overtopping. It is assumed that the along-shore resolution does not substantially affect those phenomena as long as the aspect ratio is limited to a certain value. In this study the aspect ratio of the grid y over x is 2.

Figure 4-4 shows a comparison of wave spectrum among those grid sizes. Note that the offshore wave height at 031 is calibrated (input values are slightly different for each cases) to achieve identical spectra at this location, so the difference in wave propagation depending on the resolution can be clearly identified. The comparison shows that the influence of the grid size to the wave transformation is fairly limited. Therefore, grid cells of 2 m by 4 m are used in the x and y direction, respectively.

Figure 4-4. Comparison of wave spectrum among different grid sizes.

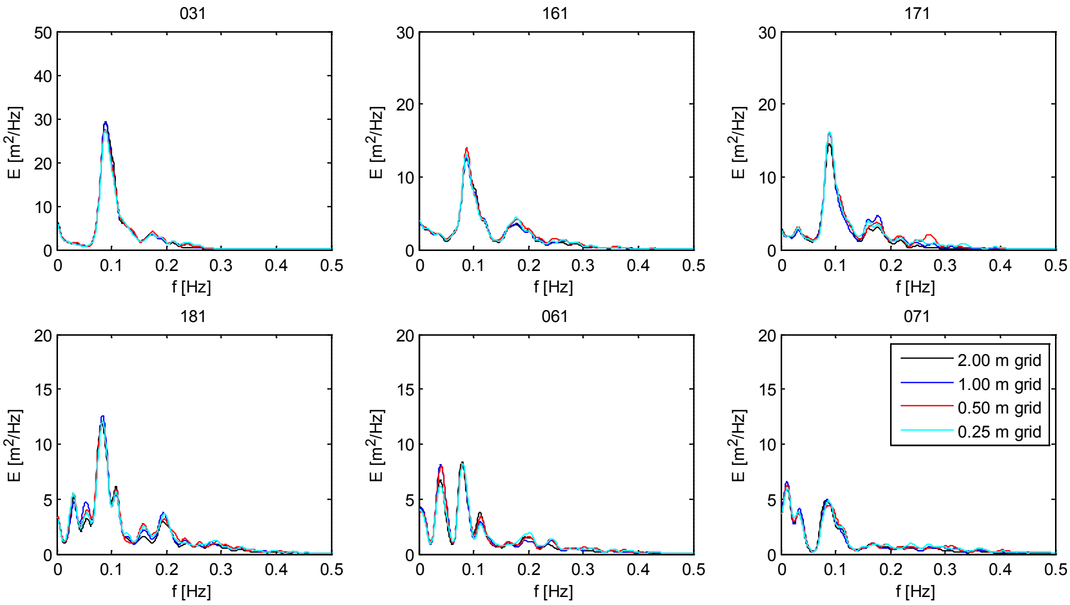

A summary of the SWASH settings is shown hereafter.

- One layer in the vertical direction
- Grid resolution 2 m in x-direction, 4 m in y-direction
- Weak wave boundary condition
- 2nd order wave generation
- Breaking ON
- FRICTION Manning n=0.019
- Non hydrostatic pressure term

SWAN model setup

Summary of the SWAN settings are shown here. Note that the boundary conditions are the same as ones used in SWASH.

- Grid resolution 1 m
- Directional wave domain CIRCLE 72
- Frequency domain 0.04 Hz to 1 Hz with 34 components
- JONSWAP gamma=1.8

- Directional spreading 22.4 degree
- 3e generation mode KOMEN
- White-capping OFF
- Triads ON
- Breaking index 0.73
- FRICTION JONSWAP coefficient $0.067 m^2 s^{-3}$
- Wave setup ON
- Triads ON

Mike21BW model setup

In this section, one-dimensional and two-dimensional simulations of waves propagating towards the dike with shallow foreshore at Petten, are performed utilizing MIKE 21 BW model. The incoming wave parameters at the inflow boundary used in all simulations are identical to the ones mentioned in Table 1 in Suzuki *et al.* (2014). Briefly, irregular wave field of JONSWAP spectrum with γ = 2.5 is used, the significant wave height, H_{m0}, equals to 4.6 m, the peak wave period T_p is set equal to 11.0 s, while the wave direction is considered normal to the dike. Note that the directional spreading of waves is not taken into account in the one-dimensional simulations, while for the two-dimensional simulations, the directional spreading angle is set equal to about 23 degrees.

Regarding the wave generation, this occurs inside the computational domain (internal wave generation), and is performed by adding the discharge of an incident wave field at a point (1D) or at a line (2D), the so-called generation line. The smallest wave period in the time series is set equal to 2 s, while the default wave generation accuracy is of first order. However, the latest release (2014) of MIKE 21 BW, includes the option of second-order corrections to the generation of incident waves. Furthermore, taking into account that the generated waves propagate in either side of the generation line and also that the open boundaries in MIKE 21 BW are fully reflective, sponge layers have to be placed next to the offshore boundary, so that the waves leaving the domain can be efficiently absorbed. The generation of irregular wave data and also the creation of a sponge layer is conducted by Mike 21 Toolbox.

As previously mentioned, the performed two-dimensional simulations refer to the case of the Petten bathymetry, which was measured on 15/11/2007 after a storm event (Figure 4-5), considering that it is uniform in the long-shore direction. The one-dimensional simulations include, except for the case of the original bathymetry, which was measured on 15/11/2007, the case of a modified (truncated) version of the same bathymetry, where spatial data above still water level are omitted (Figure 4-5). Also, in Figure 4-5, the positions of the wave buoys (031, 161, 171, 181, 061, 071) where the instantaneous free-surface elevation was measured, are shown. In all tests (1D and 2D), sponge layers are also placed at the outflow region in order to minimize the wave reflection at the outflow boundary. In the present study, sponge layers placed next to the inflow and outflow boundaries, are of length equal to 100 computational nodes, consequently the domain has to be appropriately enlarged at the inflow side. For both cases, the first of the (100) sponge layers is located at the grid point of depth +1.36 m NAP (truncation point) at the outflow region. In the following paragraph, the most important numerical parameters and calibration parameters utilized in the MIKE 21 BW, are presented.

Figure 4-5: Above: Petten bathymetry measured on 15/11/2007 and wave measurement positions.
Below: Truncated bathymetry at level +1.36 m NAP (only for 1D simulations).

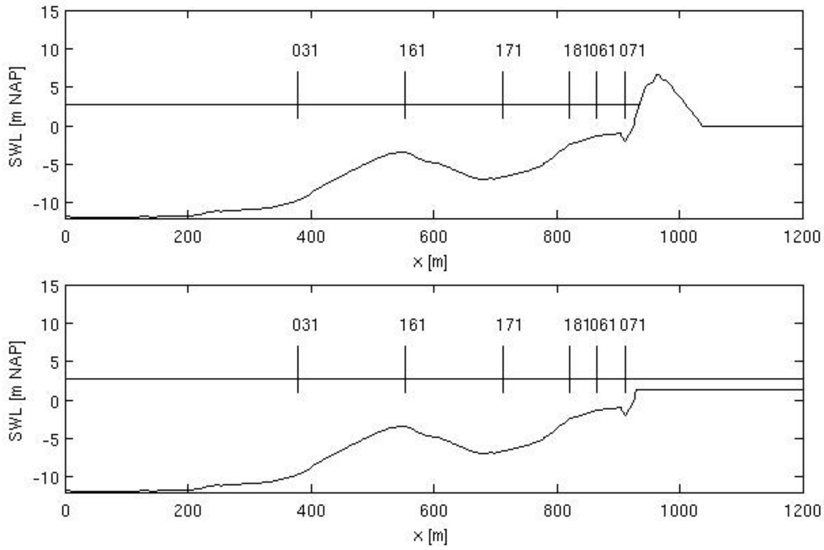

The 1DH simulations are performed on a uniform grid with size of 2.0 m, while the time-step interval is equal to 0.05 (constant), resulting into a Courant Number equal to 0.3 (< 0.5). For the 2D simulations, the grid size in the long-shore direction is considered equal to 4.0 m, while the grid size in the normal to the shore direction remained the same as in 1DH tests. A simulation period of 30 minutes is chosen so that a comparison to the available measured data and the numerical predictions of Suzuki et al. (2014) can be feasible. The bottom friction in all simulations is formulated using the Manning number which is set equal to $n = 0.019$.

One of the disadvantages of MIKE 21 BW is that wave breaking is not intrinsic in the formulation, but an incorporated feature based on the surface roller concept for spilling breakers. According to this concept, wave breaking is assumed initiated when the local slope of the free-surface elevation exceeds a certain angle (initial breaking angle, φ_B; default value = 20^o), while the gradual transition to a bore-like stage is defined by a smaller one (final breaking angle, φ_o; default value = 10^o). In the present study, for the one-dimensional tests, the initial breaking angle is set equal to 14^o, while the final one is equal to 7^o (trial and error), since these values performed better in prediction of wave energy dissipation that follows breaking. The reduction of φ_B and φ_o is also suggested in Madsen et al. (1997a; pp. 270-274) for the case of breakers over submerged bars. However, for the two-dimensional tests the default breaking values exhibited a better behavior in terms of wave energy dissipation after breaking, comparing to the utilized angles (φ_B = 14^o and φ_o = 7^o) of the corresponding one-dimensional simulations. Furthermore, sensitivity analysis for the rest breaking parameters (e.g. roller form factor) showed that, in this case, they do not affect substantially wave breaking and dissipation.

In order to simulate wave run-up, MIKE 21 BW uses the numerical treatment of the, so-called, moving shoreline (using a slot technique), which is based on the replacement of the solid bed by a permeable one characterized by a very small porosity (Madsen, et al., 1997a). This treatment is activated whenever (or wherever) the free-surface of the water intersects the bottom of the domain, and in other words results in the replacement of the physical water depth in the momentum equations by an “effective” water depth, which is determined by the vertical variation of porosity. Note that, the moving shoreline feature was activated only for the case of original bathymetry simulation. The values of the parameters used to define the porosity variation are set following the manuals recommendations: Slot depth = 5 m (default value = 4), Slot width = 0.05 (default value = 0.01), Slot friction coefficient = 0.05 (default value = 0).

The incorporation of wave breaking and/or moving shoreline in a simulation, often results into high-frequency instabilities, and for this reason an explicit low-pass numerical filter is provided by MIKE 21 BW. In the present study this filter is imposed in both of the investigated cases (original and truncated bathymetry) at the outflow region, i.e., at the intersection of water surface and the front of the dike, and specifically 6-10 grid points from the toe of the dike (towards the onshore direction) for both cases. The filter coefficient increases gradually from 0 to 0.25 within 8 grid points and then remains constant until the end of the domain (recommended values are between 0 and 1).

For the 2D simulations, the spatial discretization of the convective terms of Boussinesq equations, is achieved by a quadratic up-winding numerical scheme, with simple up-winding at steep gradients and near land. This scheme is preferred instead of the default central differencing with side feeding scheme, in order to eliminate numerical instabilities and consequently model’s blow up. Generally, the drawback of using an up-winding scheme is the resulting numerical dissipation (which also damps possible instabilities), but in the present study does not seem to affect (substantially) the numerical predictions. For the time discretization of the, so-called, cross-Boussinesq terms (spatiotemporal derivatives of fluxes in each direction) a linear time-extrapolation technique (with default factor = 1) is used by MIKE 21 BW, in order to avoid artificial dissipation of waves, resulting from the straightforward discretization (time-extrapolation factor = 0). For simulations that include wave breaking and moving shoreline it is recommended that time-extrapolation factor should be slightly less than one for numerical stability, therefore a value equal to 0.9 is chosen for the simulations included in the present study.

4.1.3 Applicability of models

SWASH and SWAN

Figure 4-7 shows wave transformation from offshore to toe of the dike. Blue, red, black, green lines show SWASH 1D calculation (i.e. the directional spreading of 0 degree), SWASH 2D calculation (i.e. the directional spreading of 22 degree) and the in-situ measurement, and SWAN 1D calculation (i.e. the directional spreading of 22 degree) respectively. Wave height is analyzed using a cut-off frequency of 0.005 Hz (Herbers *et al.*, 1995) to have a realistic value for $T_{m-1,0}$ and 0.05 Hz (Herbers *et al.*, 1995) for the separation of long waves and short waves.

The SWASH 1D calculation is conducted to see the effect of the directional spreading. As can be seen in Figure 4-7, the wave spectrum of SWASH 2D calculation shows a good correspondence with the measurement at 071 even though the value around the peak period is slightly underestimated. On the other hand, the SWASH 1D calculation is overestimated at the low-frequency part while similar spectrum to the two-dimensional calculation is obtained around the peak period. SWAN shows similar result for short waves, but it does not give any long wave output since the SWAN model cannot calculate the long wave generation.

Figure 4-6: Spatial distribution of total significant wave height (SWAN* & SWASH)

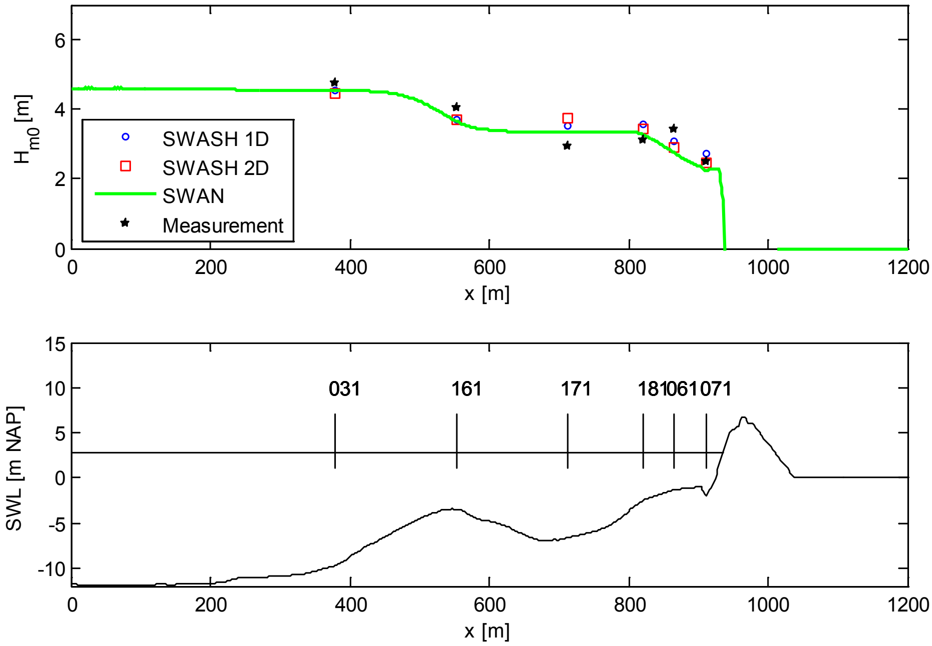

*Note that the SWAN calculation does not include reflection from the dike.

Table 4-2: Wave properties at the toe of the dike

Model [-]	H_{m0} at 071 HF [m]	H_{m0} at 071 LF [m]	H_{m0} at 071 Total [m]	$T_{m-1,0}$ at 071 Total [s]
SWASH 1D	2.18	1.61	2.71	27.0
SWASH 2D	2.23	1.04	2.46	16.7
SWAN	2.24	0.00	2.24	9.0
In-situ measurement	2.39	0.76	2.51	14.7

Figure 4-7: Wave-energy spectra computed by SWASH (1D & 2D) and SWAN at the wave-gauge positions (from 031 to 071) compared to corresponding field measurements.

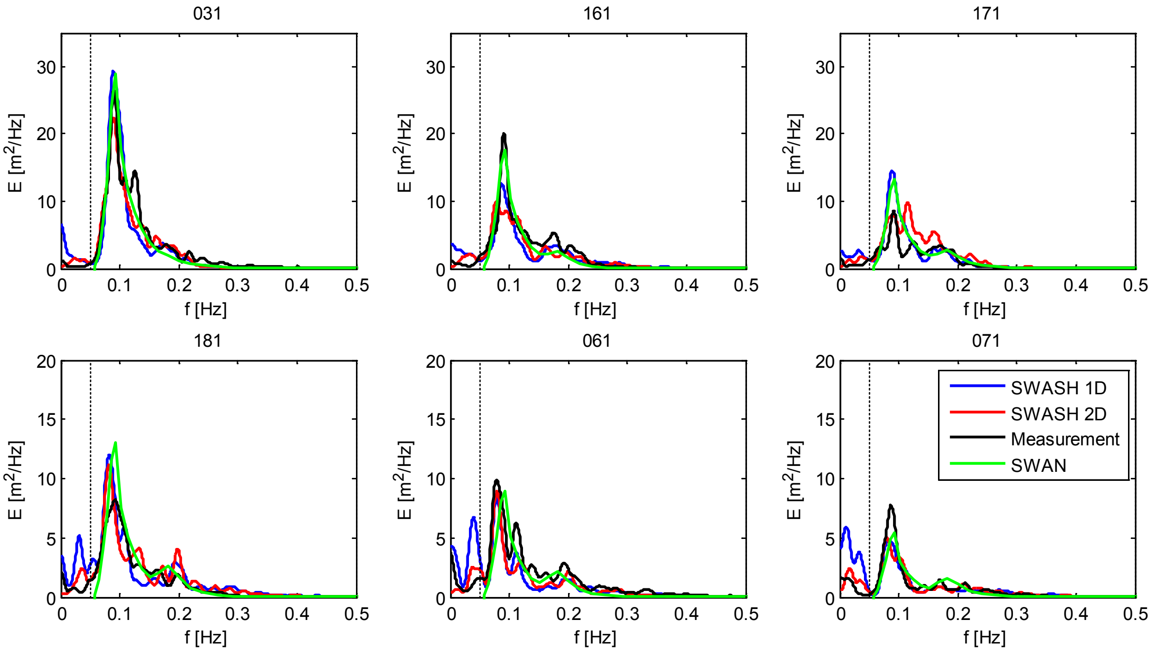

Mike21BW

Figure 4-8 shows the wave energy spectra computed by MIKE 21 BW (1D) compared to SWASH (1D and 2D) results and data corresponding to in-situ measurement. In general, MIKE's predictions seem to be close enough to SWASH results (to the 1D model), except for the one at position 061, where the predicted energy spectrum indicates a substantial underestimation of the measured peaks at each side of the peak wave period ($f_p \approx 0.1$ Hz). At the toe of the dike (position 071), the energy density of long waves is almost identical to the one of SWASH 1D, but overestimated compared to the measured one, while the measured energy peak around the peak period, which is successfully predicted by both 1D and 2D SWASH models, is not captured.

Figure 4-8: Wave-energy spectra computed by MIKE 21 BW (1D) and SWASH (1D & 2D) at the wave-gauge positions (from 031 to 071) compared to corresponding field measurements.

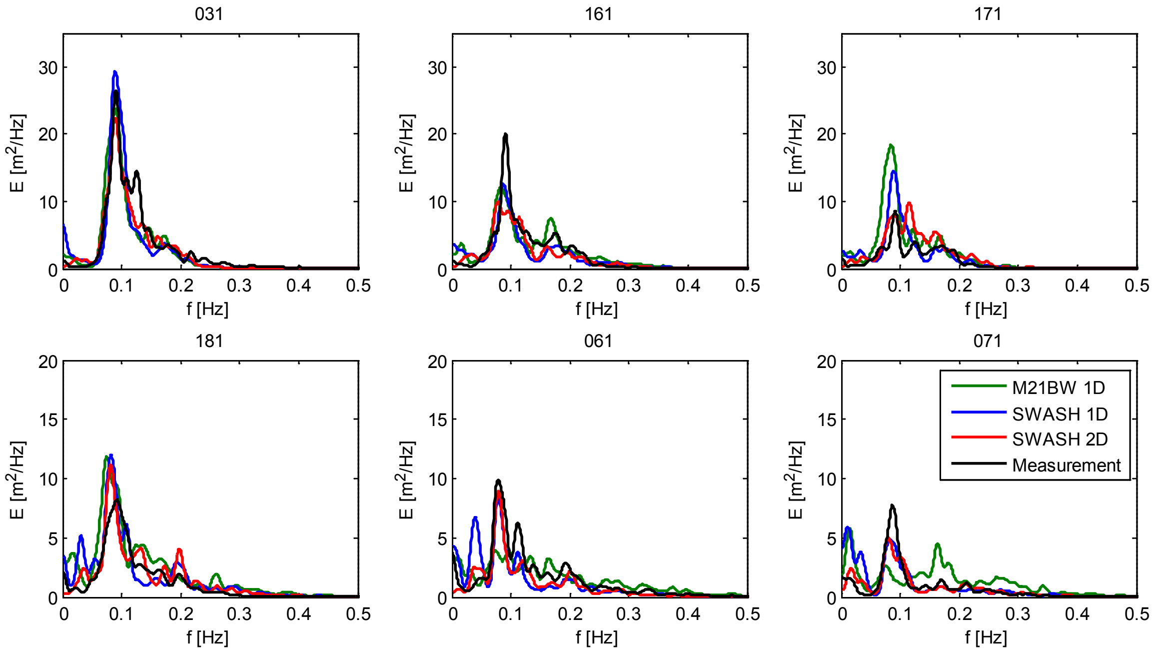

The wave energy spectra computed by MIKE 21 BW (2D) is, again, compared to SWASH (1D and 2D) results and corresponding field data, of figure 9 in Suzuki et al. (2014), as shown in Figure 4-9. In general, MIKE21-BW predictions seem to be close enough to SWASH results (especially to the 2D model, at the three last positions 181, 061 and 071), and also to the measured wave spectra (especially at positions 031, 161, 061). At the toe of the dike (position 071), the energy density of low-frequency waves is almost identical to the one of SWASH 2D, and very close to the measured one, while the measured energy peak around the peak wave period ($f_p \approx 0.1$ Hz), is underestimated by MIKE. Obviously, both SWASH predictions (1D and 2D) of the short-wave energy distribution are closer to the measured values, compared to MIKE21-BW. In general, it seems that wave directional spreading is quite important in wave transformation and wave energy dissipation in the shallow foreshore, leading to more accurate predictions for the wave climate at the toe of the dike.

Figure 4-9: Wave-energy spectra computed by MIKE 21 BW (2D) and SWASH (1D & 2D) at the wave-gauge positions (from 031 to 071) compared to corresponding field measurements.

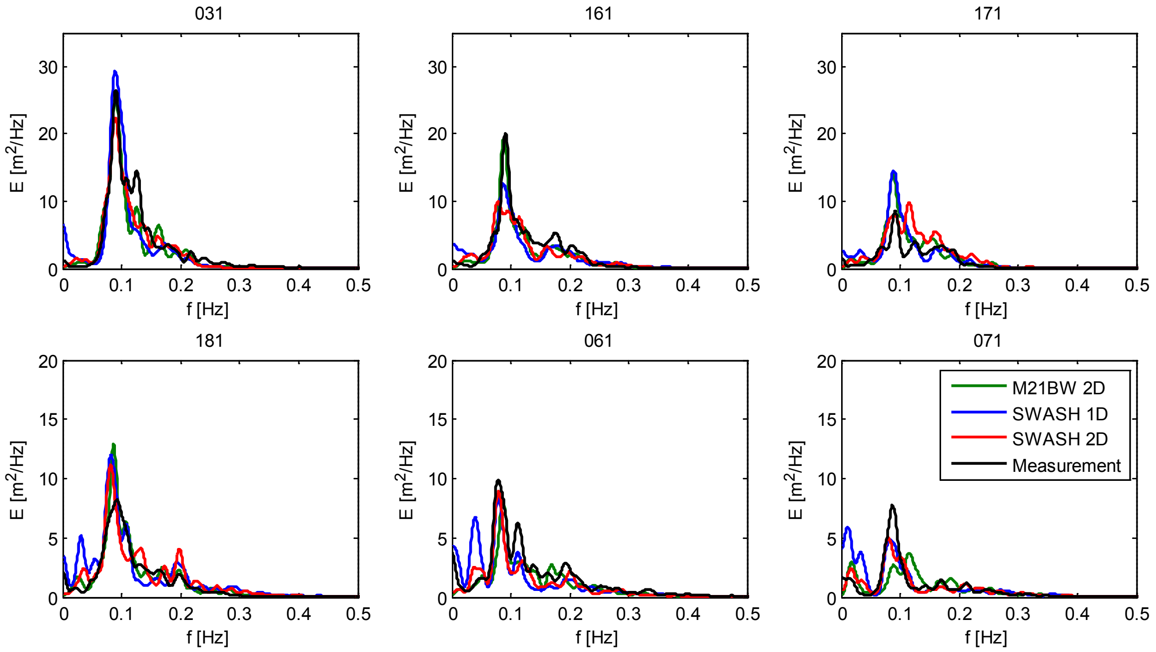

4.1.4 Computational cost

For the ‘Safety Assessment 2015’, not only the accuracy of the computation but also the computation time is important. Even though the accuracy of the computation is high, if the computational cost is too much (e.g. one run needs one day) the model cannot be used in the ‘Safety Assessment 2015’. Therefore, the computational cost also has to be discussed here.

The computational cost of all the models used here is shown in Table 4-3. As can be seen in the table, the SWASH 2D model is one of the most expensive models as the computational cost. However the computational time is about 1.5 hours by one node in a cluster (1 node 12-core machine) in “default boundary” (see Table 4-4). Even though it is more expensive than other models but it is still feasible for the ‘Safety Assessment 2015’.

Table 4-3: Computational cost for Petten simulations

Model name	**Domain size**	**Grid**	**Simulation duration**	**Computation resources**	**Computational time**
SWASH 1D	1200 m	600	30 min	Desktop PC	~1 min
SWASH 2D	1200 m x 1600 m	600 x 400	30 min	12 cores (cluster)	~1.5 h
SWAN 1D	1200 m	600	-	Desktop PC	<<1 min
Mike21BW 1D	1200 m	600	30 min	Desktop PC	~2 min
Mike21BW 2D	1200 m x 1600 m	600 x 400	30 min	Desktop PC	~2 h

To reduce the computational cost, a periodic boundary condition is applied in the SWASH 2D calculation while the default lateral boundary condition is wall condition in SWASH 2D. By introducing the periodic boundary, domain size for y direction can be shorter and still including directional spreading effect.

Table 4-4 shows the computational cost in different boundary condition in SWASH 2D. The periodic boundary reduces the computational time significantly in a fashion almost proportional to the grid reduction.

Figure 4-10 shows the spectrum for each case. Note that this calculation is different from Figure 4-7 since this calculation is without dike condition to get incident wave spectrum. As can be seen in Figure 4-10, the incident waves at the toe of the dike are almost the same: the calculation with periodic boundary condition does not change wave transformation pattern while it can reduce the computational cost. Note that some differences in the wave spectrum shape can be seen in the offshore wave gauge (e.g. 031): it is due to the randomness of wave generation of the offshore boundary. This figure shows that the randomness is reducing as progressed in the shallow zone.

Table 4-4: Computational cost in different boundary conditions in SWASH 2D.

Model name	Domain size	Grid	Simulation duration	Computation resources	Computational time
Default boundary	1200 m x 1600 m	600 x 400	30 min	12 cores (cluster)	~1.5 h
Periodic boundary	1200 m x 400 m	600 x 100	30 min	8 cores (cluster)	~ 20 min
Periodic boundary	1200 m x 400 m	600 x 100	30 min	Desktop PC	~ 2 h

Figure 4-10: Comparison of wave energy spectrum (default boundary vs periodic boundary)

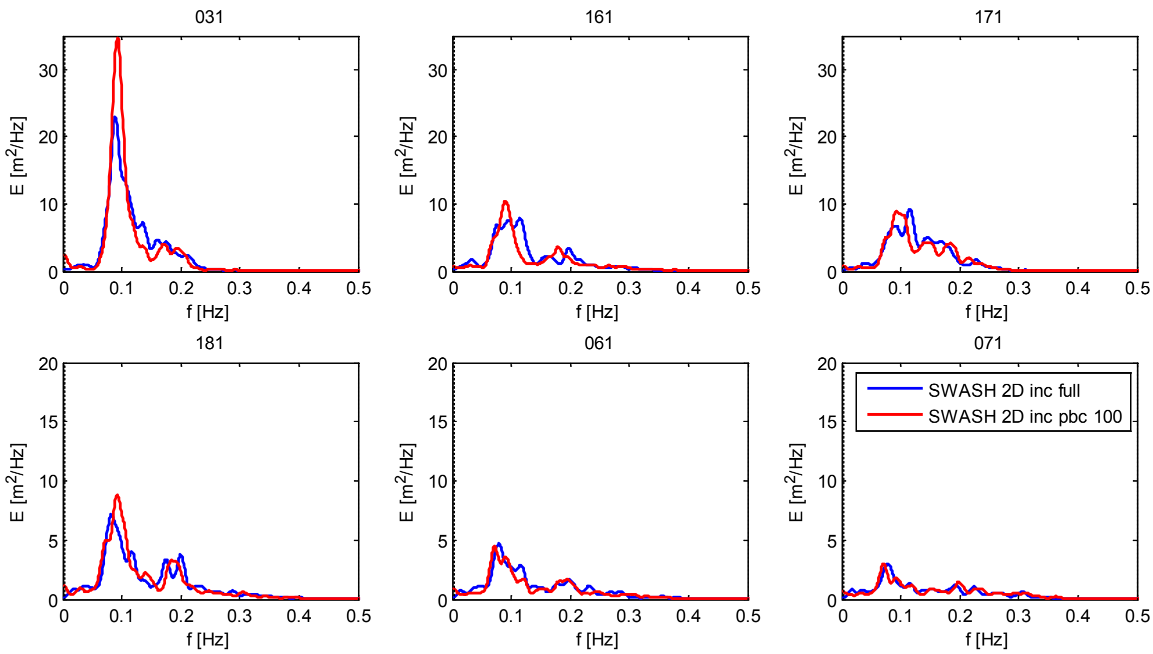

4.1.5 Conclusion

Key conclusions from the validations in this section are shown below:

- SWASH 2D represents the measured wave transformation from the field well (see wave height and wave spectrum at 071) while the wave energy around the peak frequency is slightly underestimated. The main drawback of this model is the computational cost but it can be overcome by activating the periodic boundary condition.
- SWAN reproduces short waves well while the wave energy around the peak frequency is slightly underestimated.
- Mike21-BW 1D does not accurately predicts the wave spectrum at the toe of the dike, while Mike21-BW 2D leads to much better estimation.
- SWASH and Mike21-BW predict 2D effects in a similar way (i.e.. compared to a 1D calculation, which always gives a higher frequency amplitude at the toe of the dike). Directional spreading plays an important role to reduce low frequency wave energy at the toe of dike. As Sand (1982) stated,

the amplitudes of the directional long waves seems to be significantly smaller than those of uni-directional waves, and that the wave lengths of the long waves can be altered simply by changing the directional spread of the short waves. This result reported here is also corresponding to the conclusion of Guza & Feddersen (2012), showing that the wave run-up is reduced by directional spreading.

- SWASH 2D model gives good estimations and reasonable calculation cost. On top of those, the code is open source, which means that the software is freely available (no commercial software). From the reasons above, SWASH is chosen as a wave transformation model in the 'Safety Assessment 2015'.

4.2 Extra validations for Petten sea dike case

In the last section, SWASH 2D wave transformation was validated against field measurement in Pettern. However, only one data was used for the validation using Petten data. In this section more measurement data from Petten dike are used to validate further the selected model, SWASH.

4.2.1 Model settings

Further validation for SWASH 2D is conducted using wave transformation data in November and December 2011. The bathymetry data measured on 15th November 2011, just before the events of PT2, PT3 and PT4, is available. Figure 4-11 shows the bathymetry data in the cross section of the wave buoys from 071 to 031. The wave boundary conditions used in the model runs are shown in Table 4-5. PT2 - PT4 are the further validation cases.

Figure 4-11. Topography and wave measurement positions. The bathymetry measurement was in November 2011

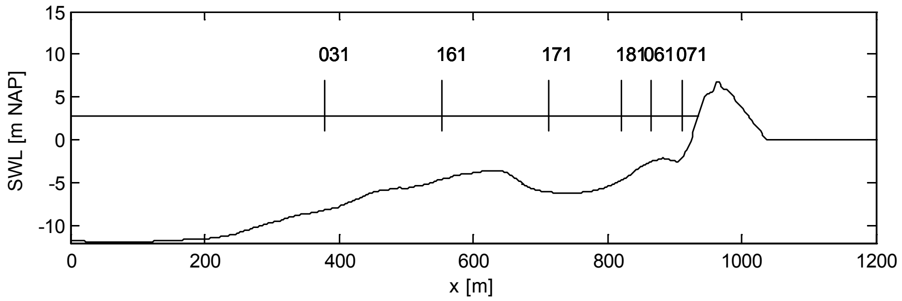

Table 4-5: The offshore wave condition employed at the wave boundary in the simulation

Code	Date	Time	SWL	H_{m0}	T_p	Dir spr.	Wav dir.	Gamma
[-]	[-]	[-]	[m NAP]	[m]	[s]	[deg]	[deg]	[-]
PT1	09/11/2007	03:20	2.82	4.6	11.0	22.4	0.0	2.5
PT2	27/11/2011	19:00	1.94	3.15	10.0	30.0	0.0	2.5
PT3	07/12/2011	17:00	1.42	4.0	11.0	30.0	0.0	2.5
PT4	09/12/2011	15:00	2.16	3.2	10.0	30.0	0.0	1.0

4.2.2 Results

Figure 4-12 to Figure 4-14 show wave-energy spectra computed by SWASH 2D compared to corresponding field measurements. In each case the information of stations 031 and 061 is missing but wave transformations from 161 to 071 are reasonably represented by SWASH 2D model, not only for short waves but also long waves.

Table 4-6 to Table 4-8 show short wave's (HF) significant wave height and long wave's (LF) significant wave height, total significant wave height and spectral period taken at 071, the toe of the dike. In each case predicted wave properties at 071 are close to the in-situ measurement values. The maximum error is within 15 % for wave height and 30 % for wave period.

Results show already good correspondence but still some differences can be explained by the uncertainties of the inputs and omitted processes. For example, the bathymetry data used in the input of PT2, PT3 and PT4 are not measured during the storm: the used bathymetries are taken at 15 November, just before the storms. Other points are wind data (wind information is not used in the numerical simulation) and current data (tidal/local current are not used in the numerical simulation).

Note that the total significant wave height and spectral wave period described here cannot be used for the wave overtopping calculation directly: incident wave properties are required.

Table 4-6: Wave properties at the toe of the dike (PT2 case)

Case [-]	Model [-]	H_{m0} at 071 HF [m]	H_{m0} at 071 LF [m]	H_{m0} at 071 Total [m]	$T_{m-1,0}$ at 071 Total [s]
PT2	SWASH 2D	2.40	0.72	2.50	11.1
	In-situ measurement	2.17	0.46	2.22	10.3

Figure 4-12: Wave-energy spectra computed by SWASH 2D compared to corresponding field measurements (PT2 case).

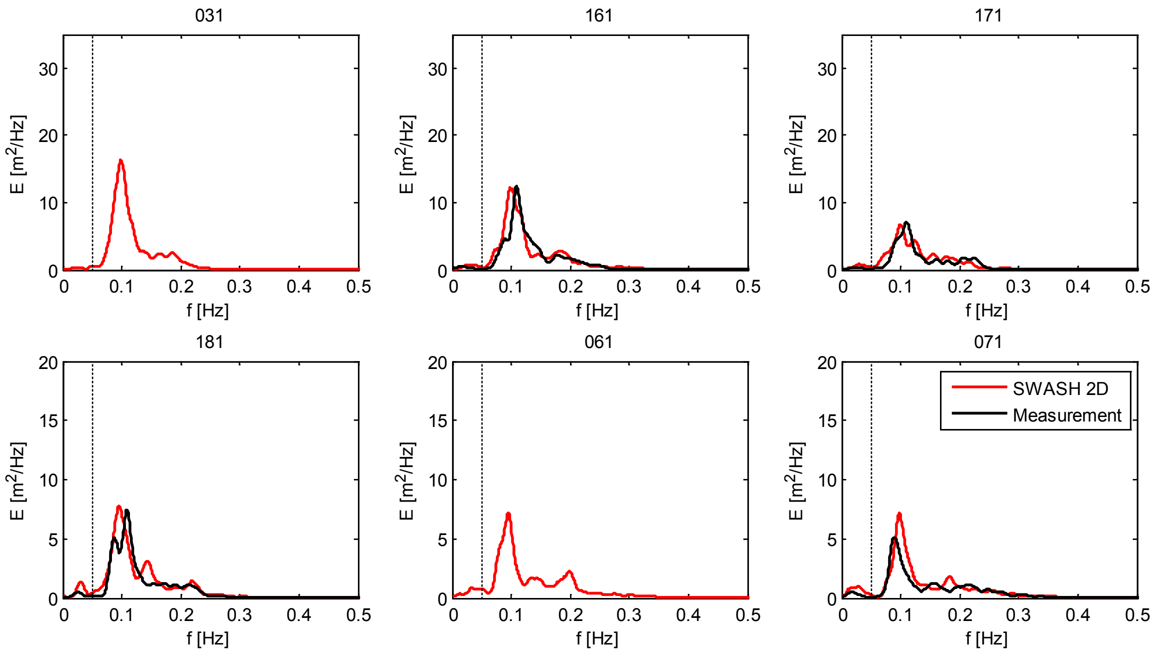

Table 4-7: Wave properties at the toe of the dike (PT3 case)

Case [-]	Model [-]	H_{m0} at 071 HF [m]	H_{m0} at 071 LF [m]	H_{m0} at 071 Total [m]	$T_{m-1,0}$ at 071 Total [s]
PT3	SWASH 2D	2.02	0.84	2.19	16.2
	In-situ measurement	2.15	0.58	2.23	12.4

Figure 4-13: Wave-energy spectra computed by SWASH 2D compared to corresponding field measurements (PT3 case).

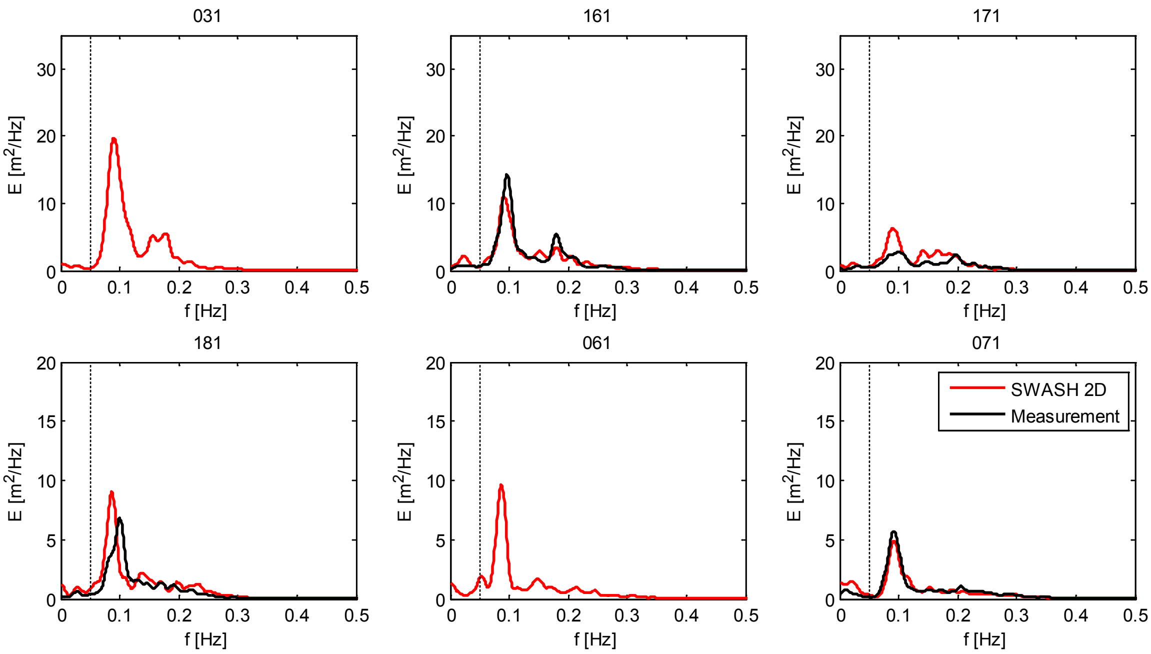

Table 4-8: Wave properties at the toe of the dike (PT4 case)

Case [-]	Model [-]	H_{m0} at 071 HF [m]	H_{m0} at 071 LF [m]	H_{m0} at 071 Total [m]	$T_{m-1,0}$ at 071 Total [s]
PT4	SWASH 2D	2.47	0.83	2.61	11.2
	In-situ measurement	2.36	0.51	2.42	10.1

Figure 4-14: Wave-energy spectra computed by SWASH 2D compared to corresponding field measurements (PT4 case).

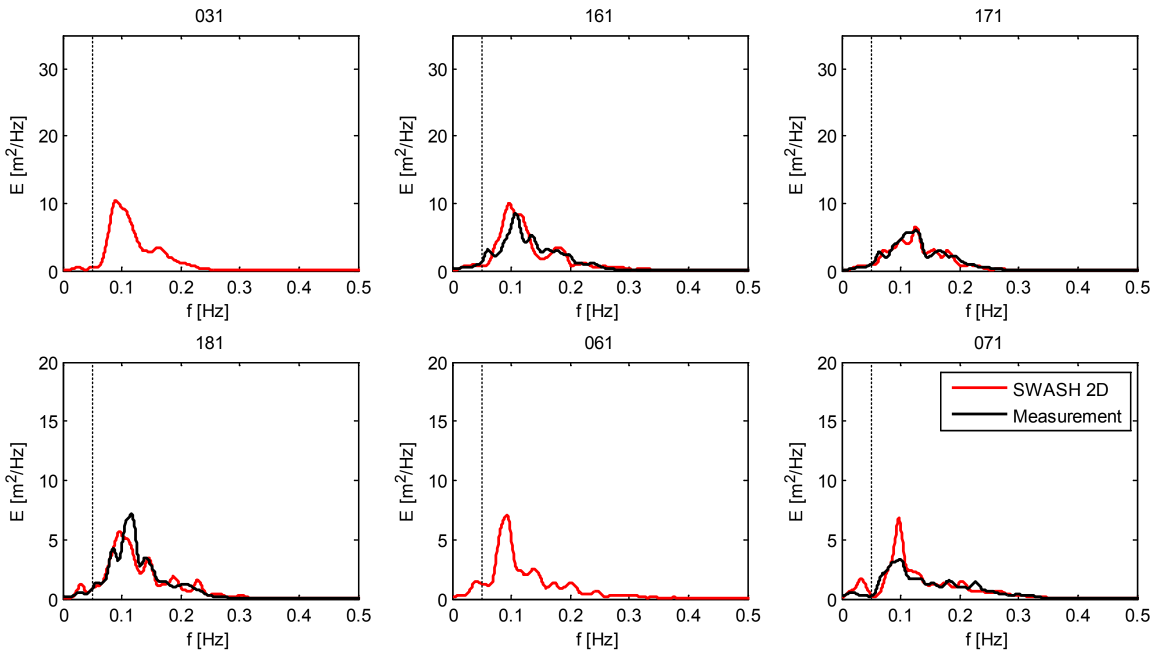

4.3 Further validation 2 (case Oostende Noodstrand)

In this section, the selected wave transformation model SWASH 2D is validated by in-situ measurements obtained at Oostende Noodstrand in 2005 (personal communication with Dr. Koen Trouw).

4.3.1 Field measurement

Coastal division conducted a field measurement campaign at Oostende Noodstrand. The wave data in the shallow zone measured in 2005 and 2006 is used to validate the selected wave transformation model SWASH 2D. The data set obtained on 16 December 2005 is used in this study.

The wave direction was measured by a directional buoy located close to -5 m TAW depth contour. The water surface time series were measured by wave buoys WTR and Sontek, whose locations are given in Table 4-9 and Figure 4-15.

The bathymetry data 9c is taken in 2005, before the storm of 16th Dec 2005. Figure 4-15 shows the bathymetry data in the cross section of the wave buoys, which direction is about perpendicular to the coast, close to NNW.

The observed data are shown in Figure 4-16. 3 time points are extracted from the modified data, 15:30, 17:00 and 18:30: every 1.5 hours. The wave transformation of those cases are calculated by SWASH 2D and SWASH 1D.

Directional spreading and wave direction is taken from Oostende Noodstrand data: in all 3 cases the directional spreading is around 30 degree in the dominant wave frequency bin, and wave direction is almost perpendicular to the coast.

Table 4-9: Position of measurement buoys

Wave sensors	X [UTM]	y	Z [m TAW]
WTR	494152.01	5676290.96	+1.27
Sontek	494021.26	5676490.92	-4.39

Figure 4-15: Geometry for the wave calculation*

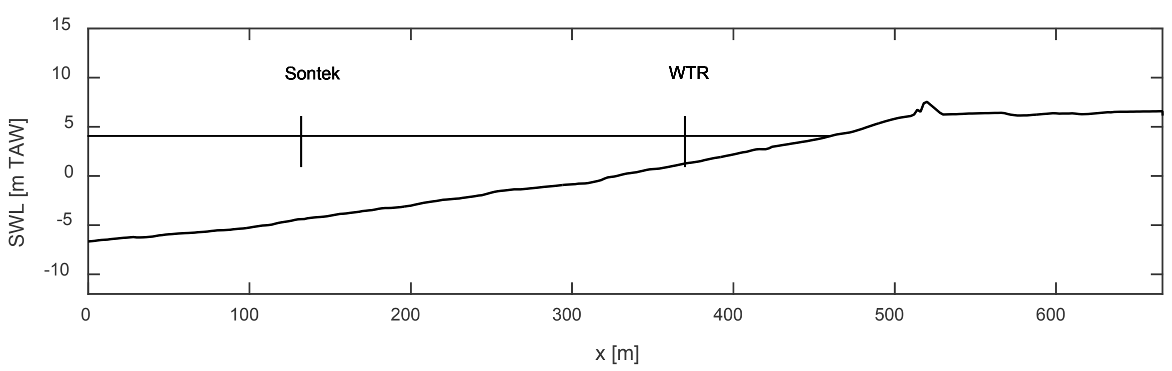

*9c configuration is selected

Figure 4-16: Time series of Hs boei, Hs WTR, Tm-1,0 WTR and tij.

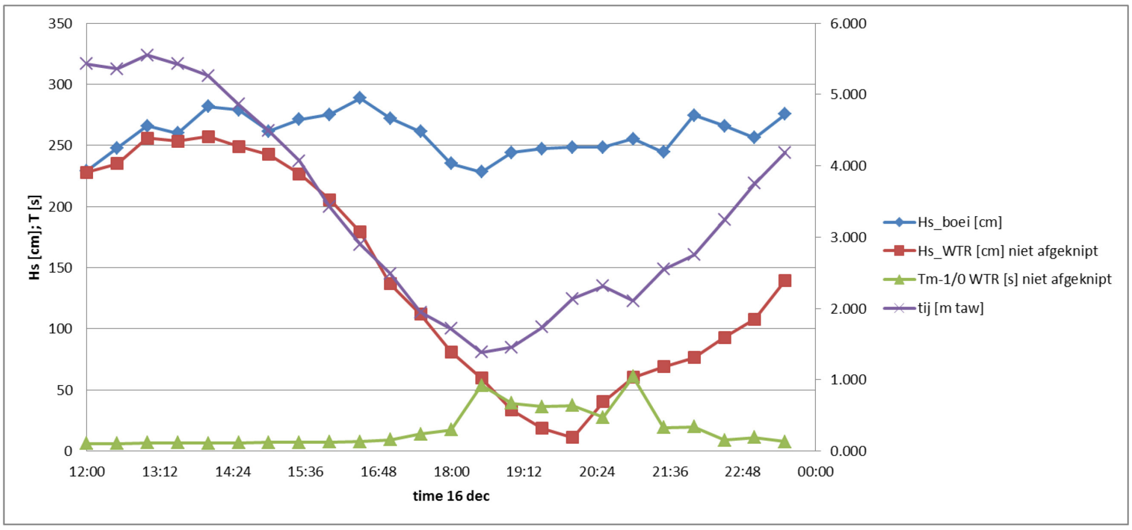

4.3.2 Model settings

Two-dimensional wave transformation calculation is conducted by SWASH (version 4.01). One layer is used for the number of vertical layers since the *kd* values for 3 cases are all less than 0.5. Grid resolution 2 m in x-direction and 4 m in y-direction is used. The wave boundary conditions used in the model runs are shown in Table 4-10. The wave generation is based on the second-order waves. A weakly-reflective boundary is applied at the wave boundary and a periodic boundary condition is applied at the lateral boundary. Since the periodic boundary condition is applied at the lateral boundary, the number of grid is in y-direction is limited to 100. This reduces the computational cost while keeping the quality of the calculation. A Manning n value of 0.019 was used as a bottom friction in the numerical model runs. The non-hydrostatic pressure term is included. The duration of the numerical simulations is 20 minutes which is the same as in the post-processing of the in-situ measurement.

Table 4-10: The offshore wave condition employed at the wave boundary in the simulation for Oostende noodstrand case

Code	Date	Time	SWL	H_{m0}	T_p	Dir spr.	Wav dir.	Gamma
[-]	[-]	[-]	[m TAW]	[m]	[s]	[deg]	[deg]	[-]
OST_1530	16/12/2005	15:30	4.07	2.7	10.0	30.0	0.0	3.3
OST_1700	16/12/2005	17:00	2.49	2.7	8.3	30.0	0.0	3.3
OST_1830	16/12/2005	18:30	1.39	2.3	10.5	30.0	0.0	3.3

4.3.3 Estimation of wave boundary condition at the toe of the dike

Figure 4-17 shows the simulated wave-energy spectrum (in red and blue) and measured wave-energy spectrum at the WTR (in black). All simulation cases with directional spreading (SWASH2D cases) show similar energy spectrum pattern compared to the in-situ measurements. Table 4-11 shows wave properties calculated from those measurement and simulations. Wave height at WTR estimated by SWASH is somewhat underestimated but this would be due to lacking of high frequency energy (OST_1530: around

0.3-0.6 Hz, OST-1700: around 0.5-0.8 Hz). This high frequency energy will be due to local wave generation by wind. SWASH1D always overestimates wave height and period compared to SWASH2D.

Figure 4-17: Wave spectrum at WTR (+1.27 m TAW)

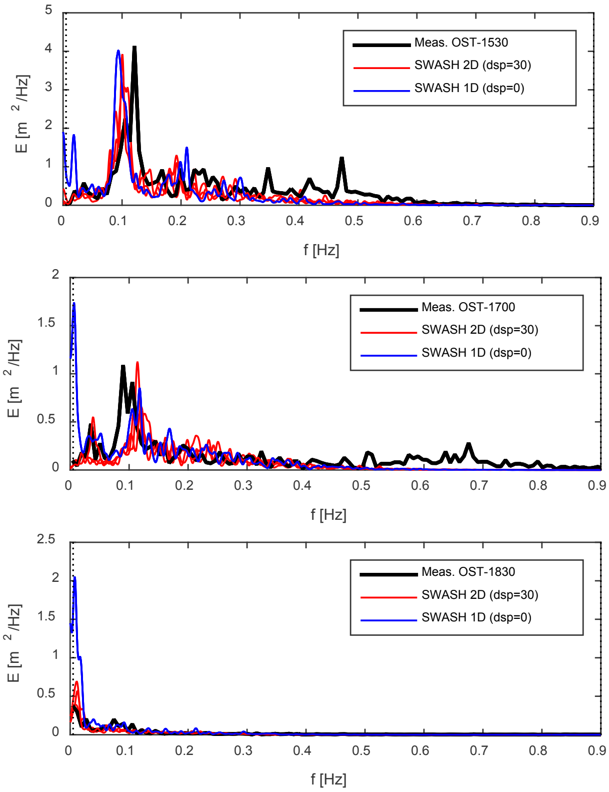

black line: measurement,
red line: 3 outputs at y=100, 200 and 300 m calculated by SWASH2D (with directional spreading 30 degree),
blue line: SWASH 1D (without directional spreading)

Table 4-11: Computed wave properties at WTR (+1.27 m TAW) by SWASH

Code	Method	H_{m0} Sontek	$T_{m-1,0}$ Sontek	H_{m0} WTR	$T_{m-1,0}$ WTR
[-]	[-]	[m]	[s]	[m]	[s]
OST_1530	Measurement	2.36	7.4	2.26	7.0
	SWASH 2D	2.51	9.1	1.83	8.6
	SWASH 1D	2.69	11.0	1.96	13.6
OST_1700	Measurement	2.06	8.2	1.36	9.3
	SWASH 2D	2.42	7.9	1.02	9.6
	SWASH 1D	2.53	10.5	1.21	27.5
OST_1830	Measurement	1.93	7.8	0.59	53.8
	SWASH 2D	2.18	9.0	0.53	47.7
	SWASH 1D	2.38	13.4	0.80	65.4

4.3.4 Computational cost

The computational cost of the SWASH 2D model is shown in Table 4-12. In this case, the simulation is conducted in a limited area, from -5 m TAW to the toe of the dike which is about 500 m. On top of that, the width is reduced by the periodic boundary condition. Therefore the computation is very short compared to the Petten case in the last section. Even by a PC, the computation is completed in 20 min in this case.

Table 4-12: Computational cost for Oostende Noodstrand simulations

Model name	**Domain size**	**Grid**	**Simulation duration**	**Computation resources**	**Computational time**
SWASH 2D	~500 m x 400 m	250 x 100	30 min	Cluster (12 cores)	4 min
SWASH 2D	~500 m x 400 m	250 x 100	30 min	PC	20 min

4.4 Conclusion

4 cases from Petten and 3 cases from Oostende Noodstrand are simulated with a 2D SWASH model. The most of the simulated wave energy show a good agreement with the measured data. The small observed differences can be attributed to differences in bathymetry (since the bathymetry was not measured simultaneously with the storm sequence), wind data (wind information is not used in the numerical simulation), current data (tidal/local current are not used in the numerical simulation) and others.

It is confirmed that the time domain model SWASH can represent wave transformation in shallow foreshore conditions (one in Petten cases, the other in Ostend cases) well. Bounded long waves are released due to wave breaking in the shallow zone and eventually free long waves are generated. This influences a lot to the wave boundary condition at the toe of the dike.

The code of SWASH is open source, which means that the software is freely available (no commercial software). In that sense SWASH is more suitable to the ‘Safety Assessment 2015’ than Mike21BW (commercial software).

From those it can be concluded that SWASH should be used in the ‘Safety Assessment 2015’ instead of SWAN used in the ‘Safety Assessment 2007’.

5 Case studies for wave transformation

5.1 Wenduine

In Chapter 4 wave transformation is validated based on in-situ measurements. However, sensitivities of several parameters have to be explored to know the characteristics of the model.

In this section, the Wenduine geometry case and its extreme wave condition at the wave boundary are used to compare the modeled wave transformation between SWASH-2D and SWAN and to perform a sensitivity analysis of the directional spreading effect and the horizontal viscosity effect.

5.1.1 Comparison with SWAN for wave transformation

Wave transformation is investigated comparing with the result of SWAN model (last methodology in the 'Safety Assessment 2007').

SWASH 2D model settings are shown below.

- One layer
- Grid resolution 2 m in x-direction, 4 m in y-direction
- Number of grid for y direction 100
- Periodic boundary condition in y direction
- Weak wave boundary condition
- Sponge layer on right side boundary (end boundary of the domain in x) 200 m
- 2nd order wave generation
- Directional spreading 0, 15, 30 degree
- Wave height & period from SWAN model
- Breaking ON
- FRICTION Manning n=0.019
- Non hydrostatic

Figure 5-1 and Figure 5-2 shows the wave transformation calculated by SWASH 2D and SWAN.

Table 5-1 shows the wave height and period at the toe of the dike in different scenario's.

SWAN shows low significant wave height at the toe. This is due to the fact that the 'Safety Assessment 2007' (IMDC, 2008) used significant wave height at the 5Hs location (i.e. 25 m from the toe). Otherwise (in the case of at the toe of the dike) the significant wave height is similar to the one obtained by SWASH. However still the wave period is underestimated in SWAN.

Table 5-1: Wave overtopping estimation in Wenduine. (crest level of 8.56 m TAW at the end of the dike)

Conditions [-]	Incident H_{m0} [m]	Incident $T_{m-1,0}$ [s]
SWASH 2D at the toe	0.87	46.9
SWAN 1D at the toe	0.39 (at x=1150m)	10.0 (at x=1150m)
SWAN 1D at the toe + Wind	0.41 (at x=1150m)	9.6 (at x=1150m)
SWAN 1D at 5H_{m0}	0.88 (**at x=1125m**)	8.7 (**at x=1125m**)
SWAN 1D at 5H_s & Wind	0.90 (**at x=1125m**)	8.5 (**at x=1125m**)

Figure 5-1: Wave height distribution (Green line: SWAN, Blue circle: SWASH 2D) without dike (incident wave information is obtained).

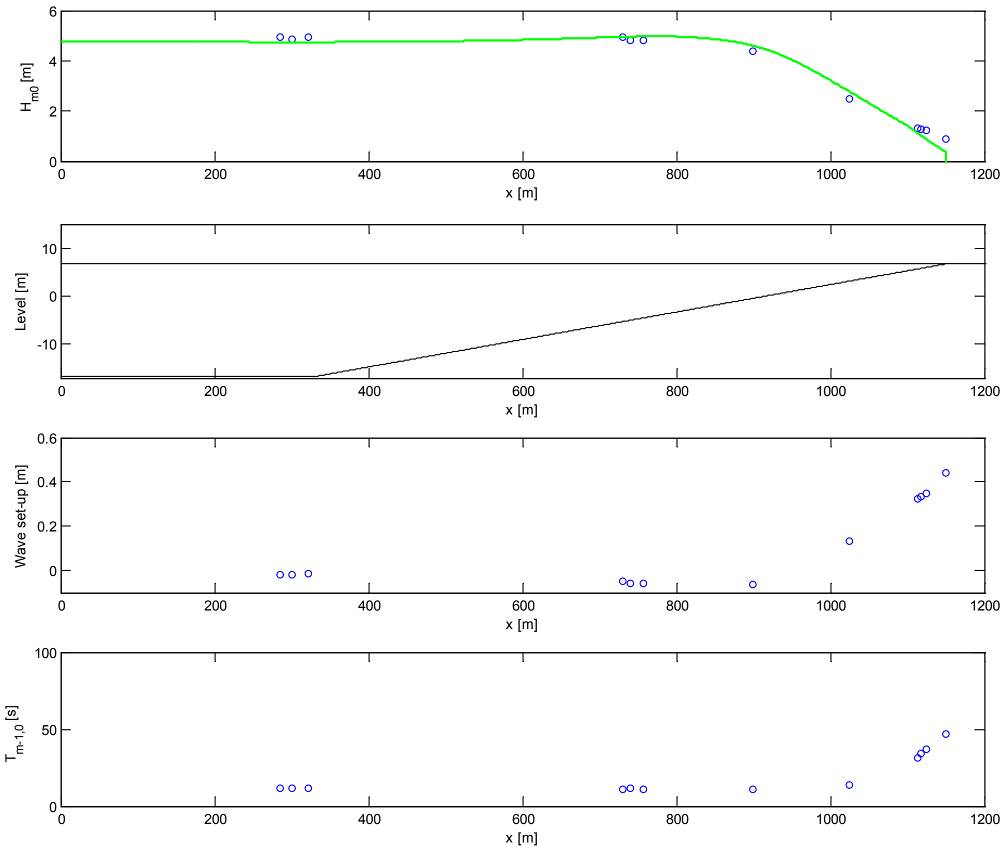

Figure 5-2: Wave spectrum (Green line: SWAN, Blue circle: SWASH 2D) without dike (incident wave information is obtained). WG position is from offshore to the toe: See Figure 5-1

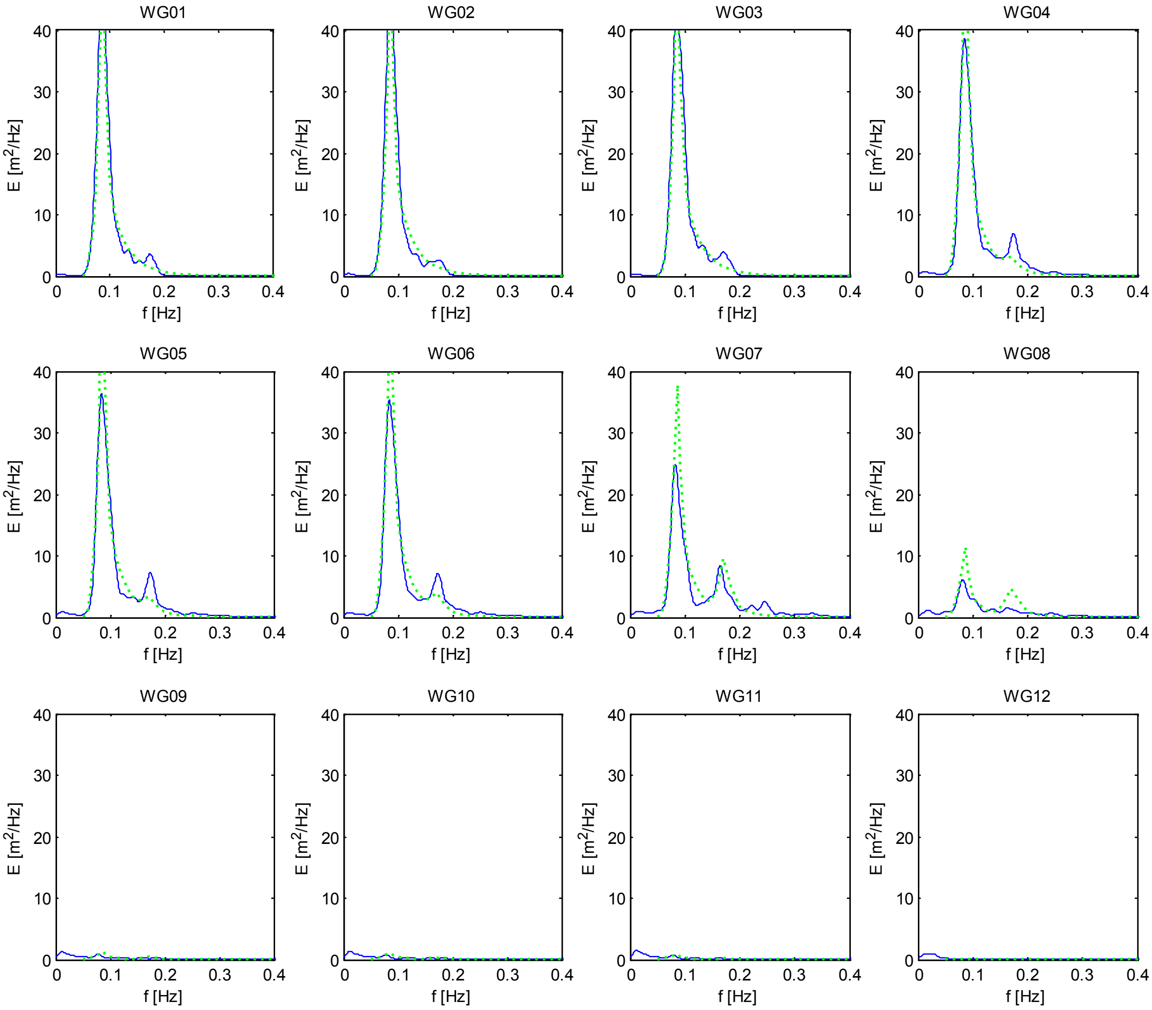

5.1.2 Directional spreading effect

One of the uncertain issues of wave transformation is directional spreading effect. Some previous studies (Guza & Feddersen, 2012; Vledder *et al.*, 2013) indicate the importance of directional spreading for wave run-up and wave transformation. The effect of directional spreading is investigated here using the example of Wenduine case by the SWASH 2D model.

SWASH 2D model settings are shown below.

- One layer
- Grid resolution 2 m in x-direction, 4 m in y-direction
- Number of grid for y direction 300
- Periodic boundary condition in y direction
- Weak wave boundary condition
- Sponge layer on right side boundary (end boundary of the domain in x) 200 m
- 2^{nd} order wave generation
- Directional spreading 0, 15, 30 degree
- Wave height & period from SWAN model
- Breaking ON
- FRICTION Manning 0.019
- Non hydrostatic

Figure 5-3 shows spatial distribution of significant wave height, wave period and wave set-up for 3 different directional spreading (0, 15 and 30 degree) calculated by the SWASH 2D model. Table 5-2 shows significant wave height, wave period and wave set-up at toe of the dike for 3 different directional spreading (0, 15 and 30 degree) calculated by the SWASH 2D model. Figure 5-4 shows spectrum at each measurement location.

As shown in Table 5-2 and Figure 5-4, different directional spreading gives different results at the toe of the dike. Not only wave height but also wave period becomes smaller when directional spreading is included in the calculation.

It is important to take into account the directional spreading for the estimation of wave properties at toe of the dike to be used for the wave overtopping calculation.

Figure 5-3: Spatial distribution of Hm0, wave set-up and spectral period for different directional spreading (0, 15 and 30 degree)

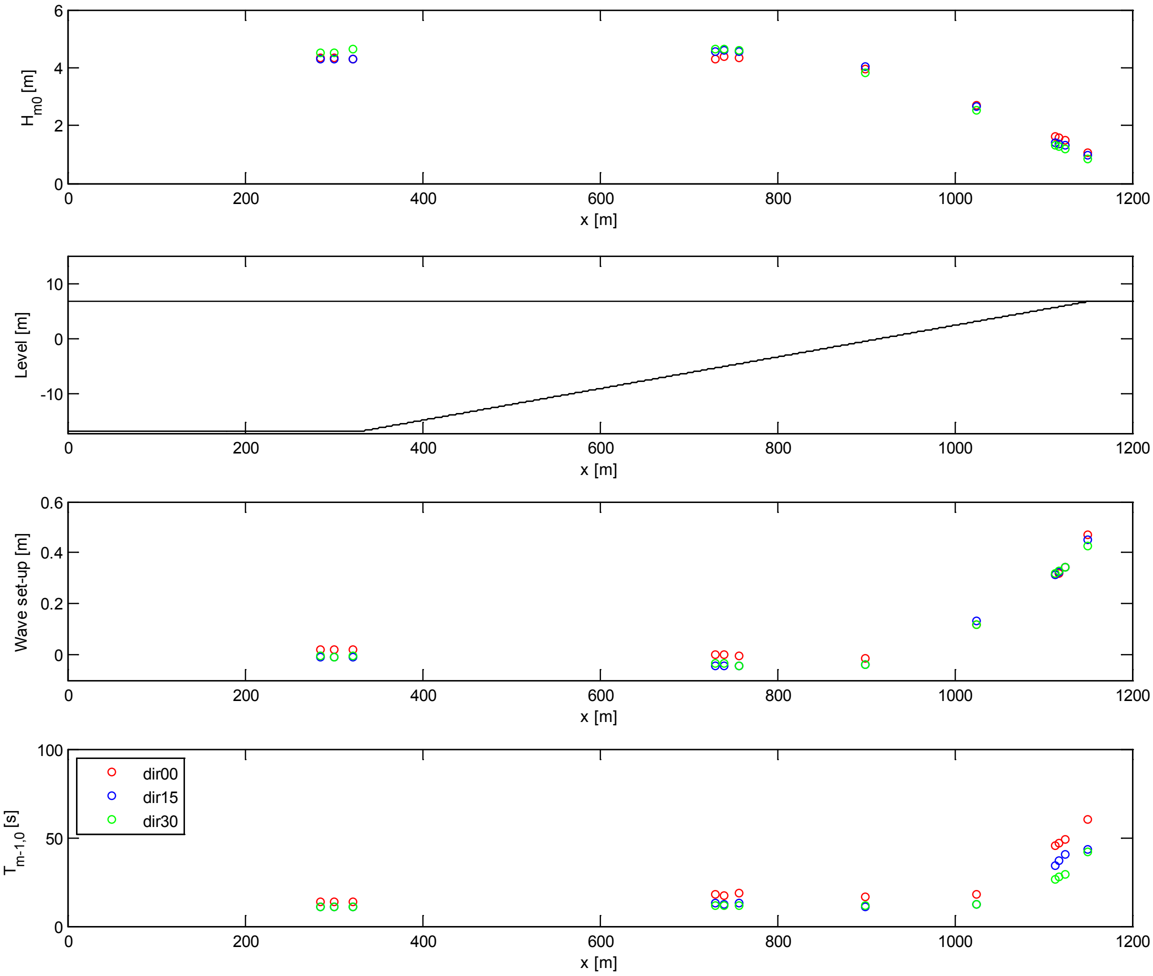

Table 5-2: Hm0, wave set-up and spectral period for different directional spreading (0, 15 and 30 degree)

Direcitonal spreading	Incident H_{m0} at 071	Incident $T_{m-1,0}$ at 071	Wave set-up at 071
[-]	[m]	[s]	[m]
Directional spreading 0 deg	1.06	60.3	0.47
Directional spreading 15 deg	0.96	43.2	0.45
Directional spreading 30 deg	0.86	41.7	0.43

Figure 5-4: Wave spectrum for different directional spreading (0, 15 and 30 degree)

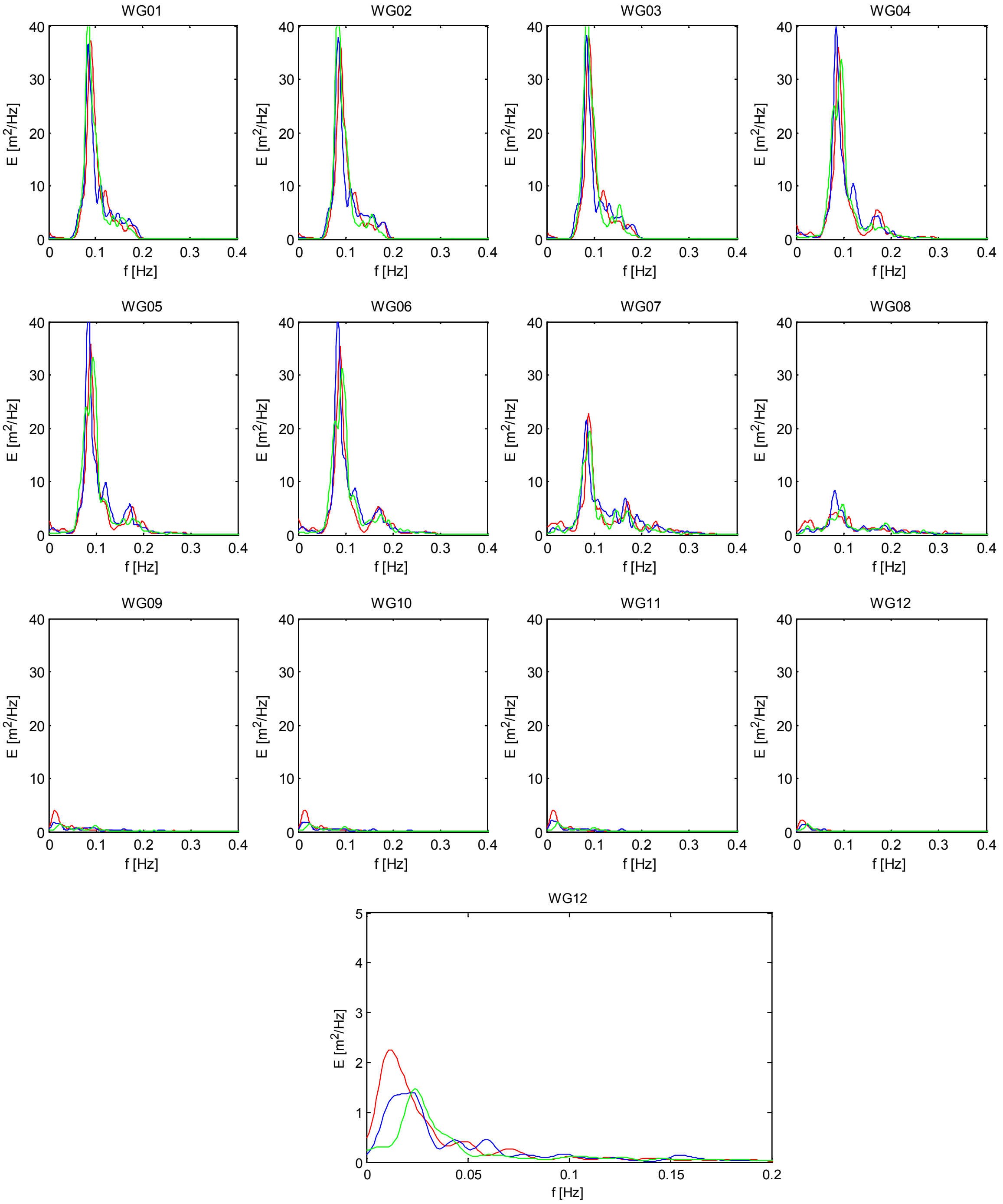

5.1.3 Horizontal viscosity effect

In this section, the effect of horizontal viscosity, which is an option of SWASH 2D input, is investigated. By activating horizontal viscosity (i.e. default constant viscosity, see The SWASH team, 2016), dissipation by a horizontal eddy can be simulated.

Based on this result, a decision is made whether if it is used or not for the 'Safety Assessment 2015'.

Figure 5-5 shows wave spectrum with and without horizontal viscosity. The horizontal viscosity does not affect to the wave transformation so much and final value of wave height and period stay the same at the toe of the dike in this case.

However, the most important effect to use horizontal viscosity is to introduce more dissipation in the domain, which stabilizes the computation. By using horizontal viscosity, the calculation became much more stable.

Figure 5-5: Wave spectrum with and without horizontal viscosity

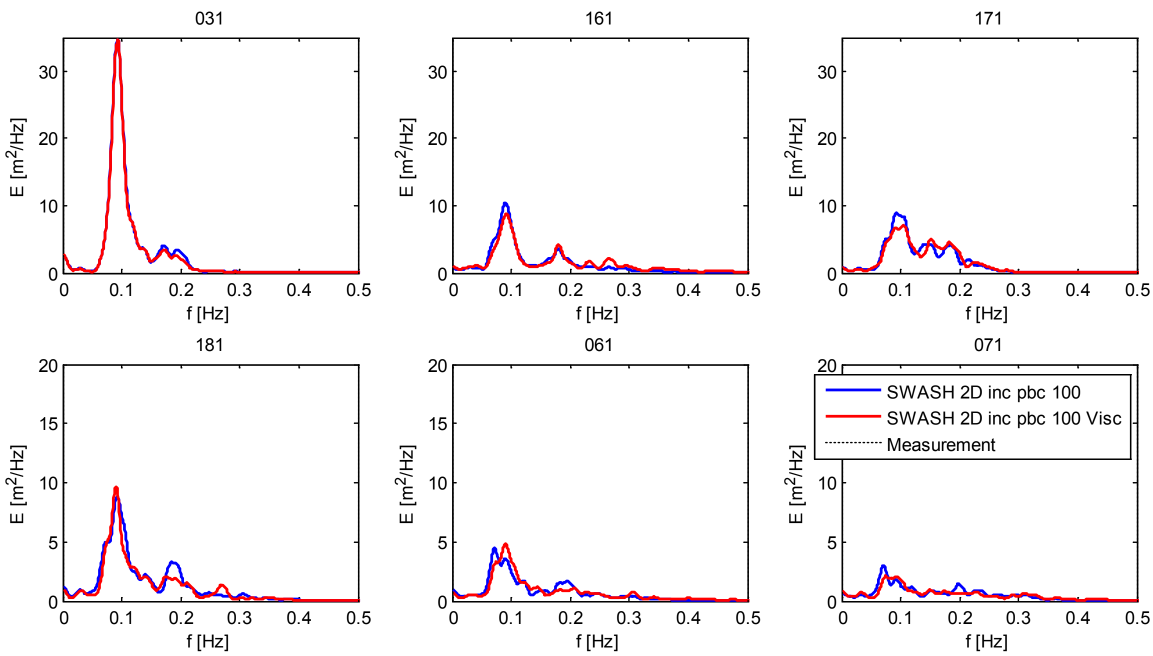

5.2 Special cross sections & Koksijde

5.2.1 Wave transformation in special cross section

Wave transformation is calculated for special geometries, which exists in the Flemish coast. The 3 geometries are 1) small sand berm case, 2) long berm case and 3) short berm case. All the foreshore slopes are almost the same ~1/50 and toe of the dike location is all same at +6.5 m TAW (Figure 5-6). The bathymetry is extended to -15 m TAW to avoid the boundary effects. Wave boundary condition is based on a simplified extreme condition: H_{m0}=5 m, T_p=12 s and directional spreading of 15 degree. In this section, only wave transformation for those special cases is investigated.

Incident wave at the toe of the dike is calculated by using a bathymetry which is flat after the toe position. In this method the difference behind the toe does not affect to the incident wave properties. Therefore incident wave in long berm case and short berm case are exactly the same since bathymetry up to the toe is the same.

Figure 5-7 and Figure 5-8 show wave energy spectrum at -5 m TAW and toe of the dike. As can be seen in the figures, all the energy is concentrated at the low frequency side. Figure 5-9 and Figure 5-10 show spatial distribution of wave properties for both cases. Those result will be used for the overtopping calculation in Chapter 7.

Figure 5-6: Special cross sections tested in SWASH 2D.

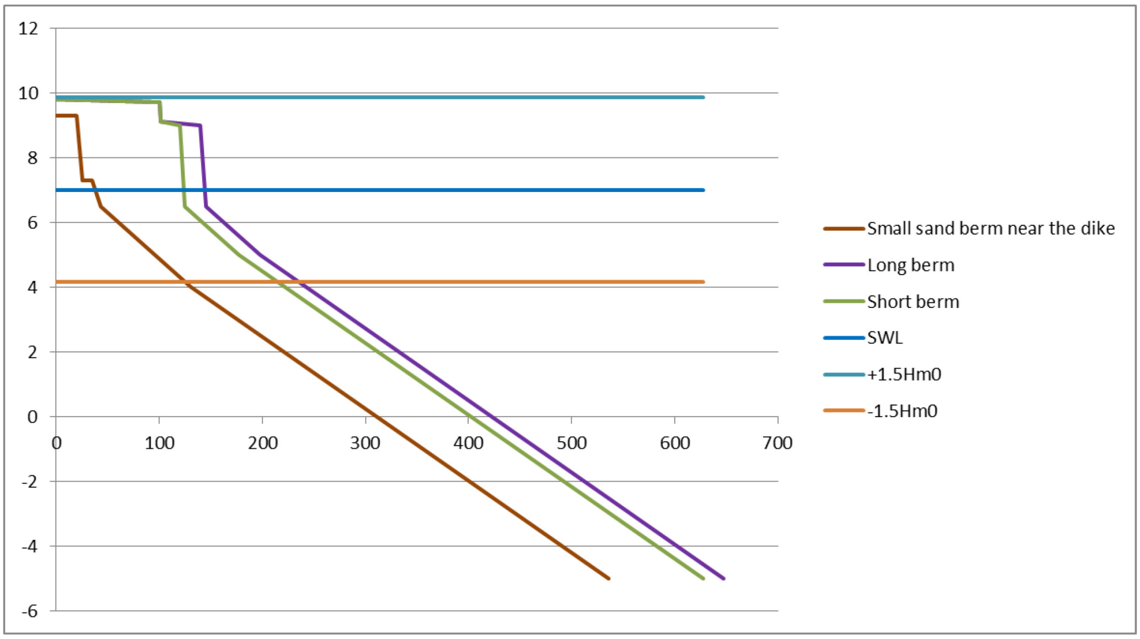

Figure 5-7: Wave energy spectrum calculated in SWASH 2D (small sand berm case).

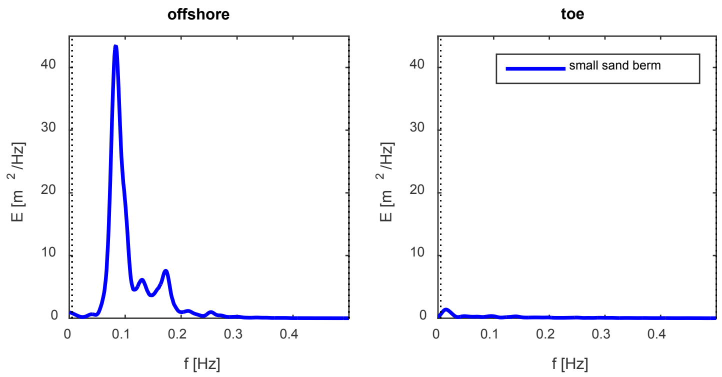

Figure 5-8: Wave energy spectrum calculated in SWASH 2D (long and short berm case).

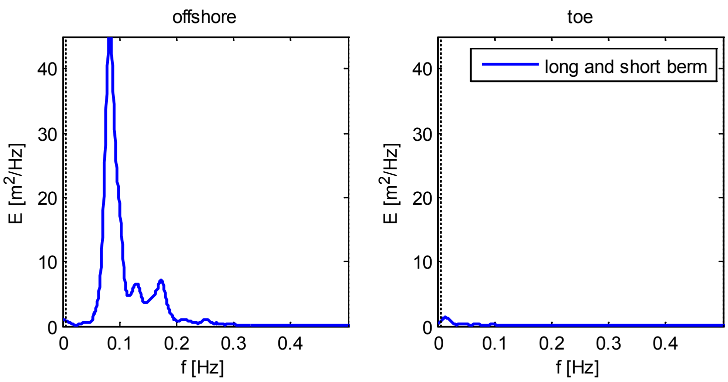

Figure 5-9: Wave properties calculated in SWASH 2D (small sand berm case).

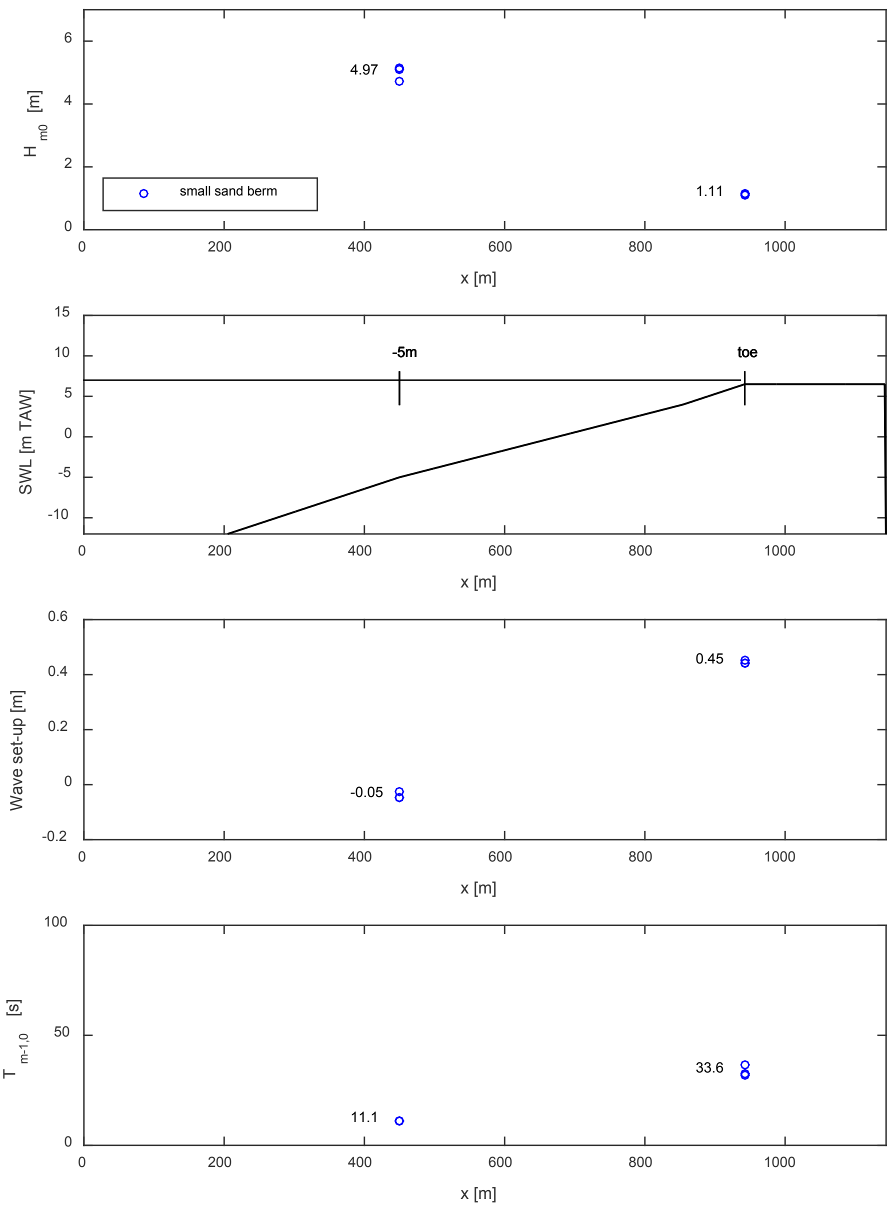

Figure 5-10: Wave properties calculated in SWASH 2D (long and short berm case).

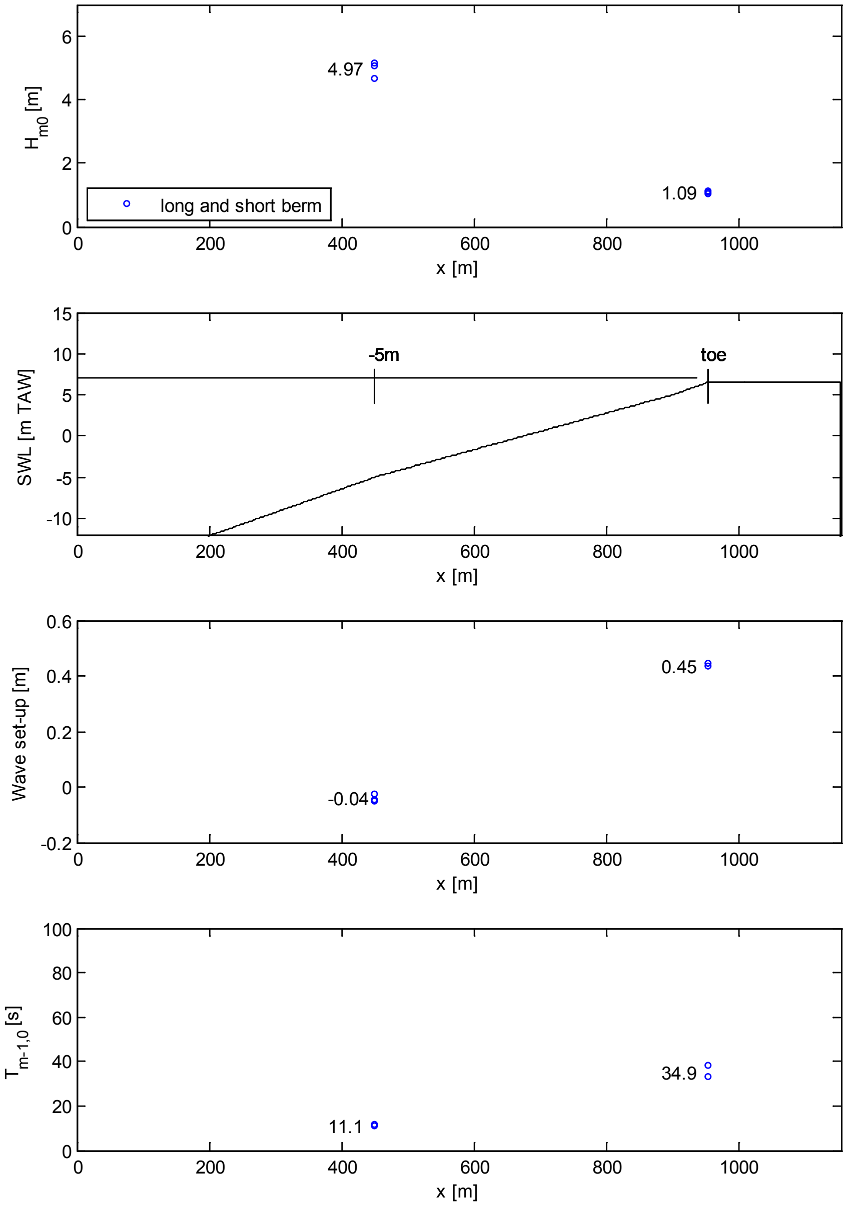

5.2.2 Wave transformation in Koksijde

The wave transformation is calculated for Koksijde. This geometry has one of the lowest toe levels in the entire Flamish coast, around +5 m TAW. Wave boundary condition is based on simplified extreme condition: H_{m0}=5 m, T_p=12 s and directional spreading of 15 degree.

The incident wave at the toe of the dike is calculated by using a bathymetry which is flat after the toe position.

Figure 5-11: Wave energy spectrum calculated in SWASH 2D (Koksijde case). Figure 5-11 shows the wave energy spectrum at -5 m TAW and toe of the dike. As can be seen in the figures, most of the energy is concentrated at the low frequency side even though it is one of the lowest toe levels. However this toe level is calculated by Durosta, it can be deeper in the 'Safety Assessment 2015'. Figure 5-12 show spatial distribution of wave properties for both cases. Those result will be used for the overtopping calculation in Chapter 7.

Figure 5-11: Wave energy spectrum calculated in SWASH 2D (Koksijde case).

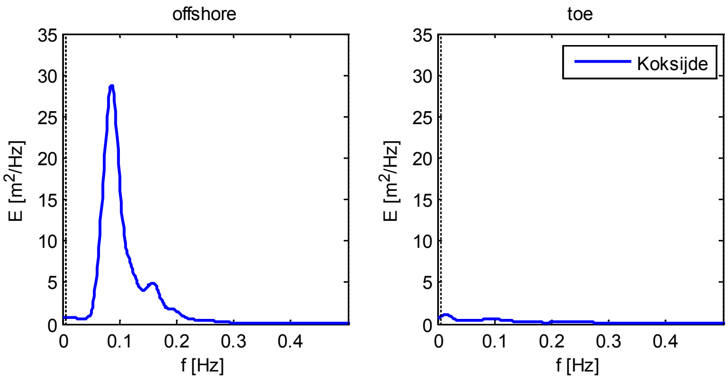

Figure 5-12: Wave properties calculated in SWASH 2D (Koksijde case).

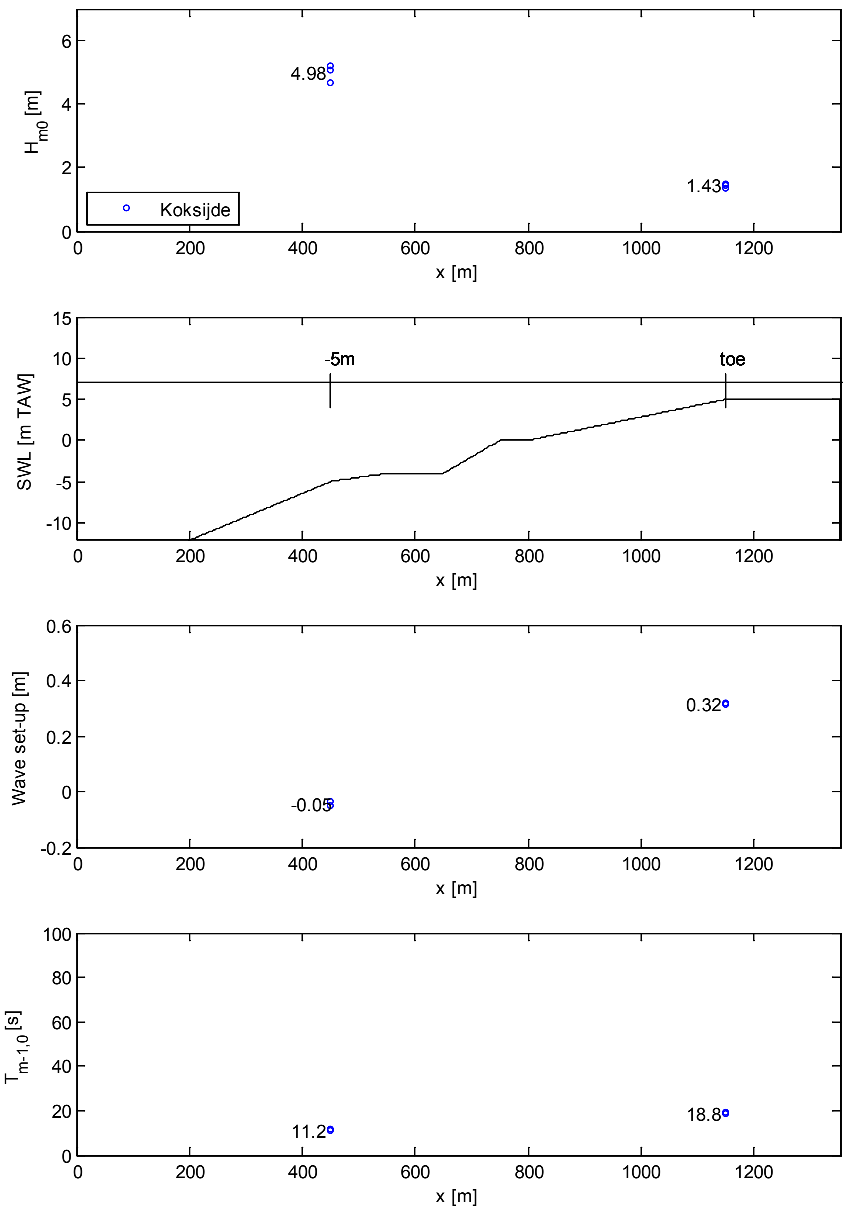

5.3 Conclusion

In this section, the SWASH model is applied to the case of Wenduine, some special cross sections and Koksijde. First the difference between the SWAN model and the SWASH model is investigated in the Wenduine configuration in order to see the difference between the 'Safety Assessment 2007 and 2015'. Additionally, the sensitivity of the model results to the effect of directional spreading and horizontal viscosity is tested. Next, wave transformation calculations are conducted for special cross sections and Koksijde in order to use them for overtopping calculation in section 7.

Key conclusions obtained from the analysis in this section are shown below.

- SWAN is underestimating the wave properties at toe of the dike compared to SWASH. Nevertheless, the incident wave height value obtained with the 'Safety Assessment 2007' is comparable to the one obtained with the 'Safety Assessment 2015', due to the difference of the toe position. It is located at the toe (in the simplified Wenduine bathymetry, 1/35 foreshore slope and ½ dike slope) in the 'Safety Assessment 2015' while 25 m offshore point from the toe is used in the 'Safety Assessment 2007'. Note that the exact definition of the toe position in the 'Safety Assessment 2015' is defined in Suzuki et al. (2016).
- Wind effect is tested in SWAN, however the influence of the wind for wave height is limited. Therefore wind is not included in the methodology for the 'Safety Assessment 2015'. Note that the influence of the wind for the wave set up in SWASH can be investigated in the future.
- Specifying an appropriate degree of directional spreading is important for the accurate estimation of wave properties at the toe of the dike.
- Horizontal viscosity effect is also tested and we found that the influence of the horizontal viscosity is limited in this configuration (1/35 foreshore slope). It will still be activated in the 'Safety Assessment 2015' since it might have influence in different configurations, and stability of the computation will be slightly better.

6 Validation of wave overtopping calculation by SWASH

6.1 Petten case

In this section, wave overtopping calculation is conducted by 2 methodologies; SWASH 1D overtopping calculation and EurOtop (2007) method. The SWASH 1D overtopping calculation means to calculate overtopping discharge by SWASH 1D using layer thickness and flow speed on the crest, based on the wave boundary condition at the toe of the dike calculated by SWASH 2D. Thus the directional spreading effect is included. One of the drawbacks of this method is that a calibration has to be conducted to adjust input of SWASH 1D to the output of SWASH 2D. Note that a full 2D SWASH calculation for overtopping is not possible due to stability issues.

6.1.1 Settings and validation

For the overtopping calculation by SWASH 1D using layer thickness and flow speed in time domain model, smaller dx is necessary: in the Petten configuration (i.e. a case dominated by short waves) dx should be smaller value than 2 m to maintain quality of the wave overtopping calculation in this study (Suzuki et al., 2014).

First the grid size of 0.5 m in x-direction and 0.5 m in y-direction is tested to see if 'SWASH 2D overtopping calculation' (in this 2D calculation, both wave transformation and wave overtopping are calculated) is possible. However, due to the instability of the computation, the result has not been obtained. It seems that the computation becomes more unstable when the grid size becomes smaller. Since the computation is not completed due to the instability of the model, an alternative method is proposed here. That is a combination of 2D calculation and 1D calculation: the 2D calculation is used for the wave transformation and the 1D calculation is used for the wave overtopping.

From the sensitivity analysis, the wave transformation does not change so much in the different grid size. However, the wave transformations in the 1D and 2D are different in the shallow foreshore case as can be seen in the difference in the spectrum at 071 in Figure 4-7. Therefore it is important to use 2D model to obtain better boundary condition at the toe of the dike.

After the 2D calculation, the 1D model is calibrated to be able to reproduce the wave spectrum at the toe of the dike. A straightforward calibration procedure is obtained by iteratively adjusting the incident wave height at the wave boundary in small steps to obtain a certain energy spectrum at the toe of the dike. Thanks to the existence of the slope the spectrum shape become similar to the target (measured) one. The result of the calibration is shown in Figure 6-1. The spectrum obtained from the two-dimensional model is now reproduced by the 1D model well while it is not perfect reproduction. Probably 3-5 runs will be needed to tune the target settings (wave properties has to be adjusted within an acceptable range, which is defined in the 'Safety Assessment 2015' as +-3% error in H_{m0}, +-5% in $T_{m-1,0}$.and +-5cm in mean water level at the toe of dike). The bottom friction is set as zero.

6.1.2 SWASH 1D overtopping calculation result

The calculated wave overtopping result is shown in Table 6-1. Depending on the wave train, the wave overtopping discharge changes a lot: sometimes factor 10 between SWASH estimations. The wave overtopping discharge is 2.6 l/s/m (dx=0.5 m is used, averaged 5 wave trains) and 1.5 l/s/m (dx=0.1 m is used, averaged 5 wave trains) whereas the wave overtopping discharge from the in-situ measurement is 1.4 l/s/m. It seems the model reproduces the wave overtopping discharge very well.

However, the number of wave overtopping events is underestimated: the number of the wave overtopping is 7.0 times/20 minutes (dx=0.5 m) and 7.4 times/20 min (dx=0.1 m) whereas the wave overtopping discharge from the in-situ measurement is 25 times/20 minutes (Figure 6-2).

Table 6-2 shows measured overtopping discharge in the different time (PT2-4) and the number of the overtopping. As can be seen here, number of wave overtopping can be smaller in other condition (e.g. 2.1 l/s/m and 14 times). Those differences has to be investigated further in a future study. Note that the aforementioned aspects could also play a role in the difference between modeled and measured overtopping differences in bathymetrical data (bathymetry data are not exactly the same: the used bathymetries are taken at a certain moment, not during the storms used in this validation), wind data (wind information is not used in the numerical simulation), current data (tidal/local current are not used in the numerical simulation), etc.

Table 6-3 shows Wave overtopping discharge in different wave trains using 500 waves. It is clear that the scatter of the overtopping discharge is drastically reduced.

Figure 6-1: Calibrated the wave spectrum (blue line) at the toe of the dike.

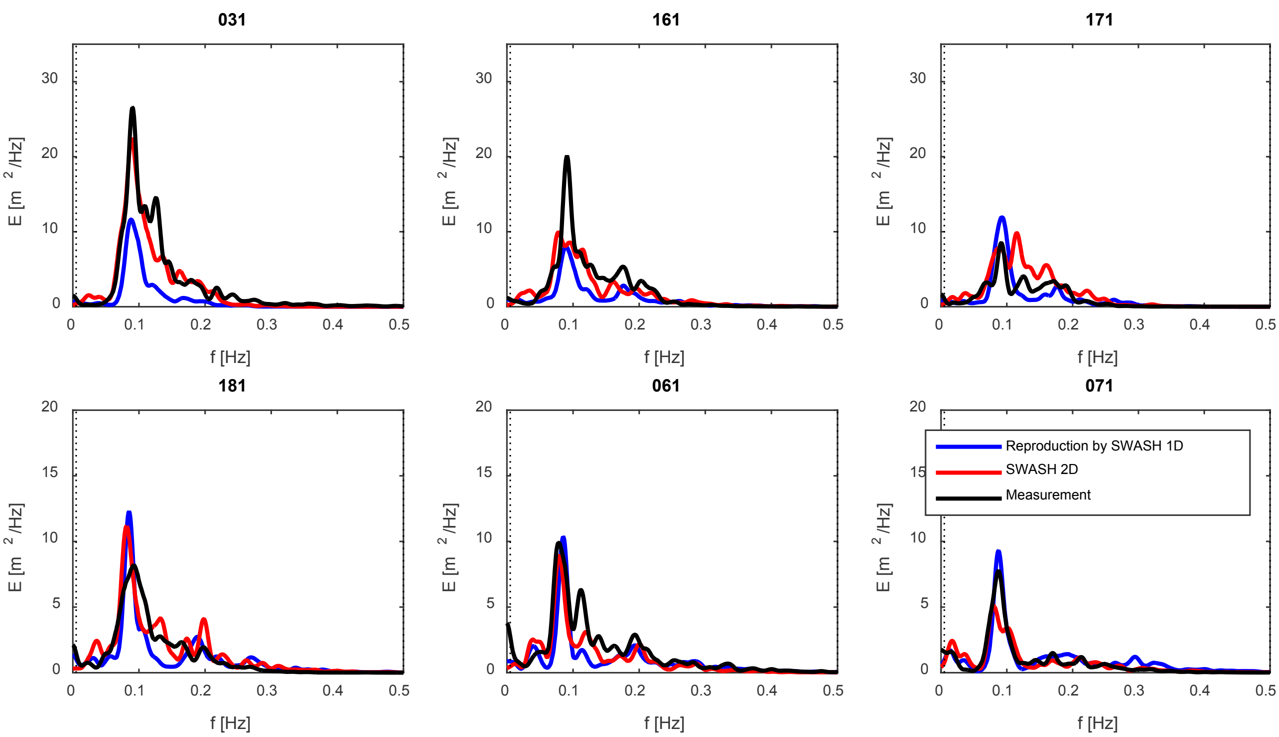

Figure 6-2: Overtopping volume per times (individual overtopping) at 3:20 on 9/11/2007, 25 times.

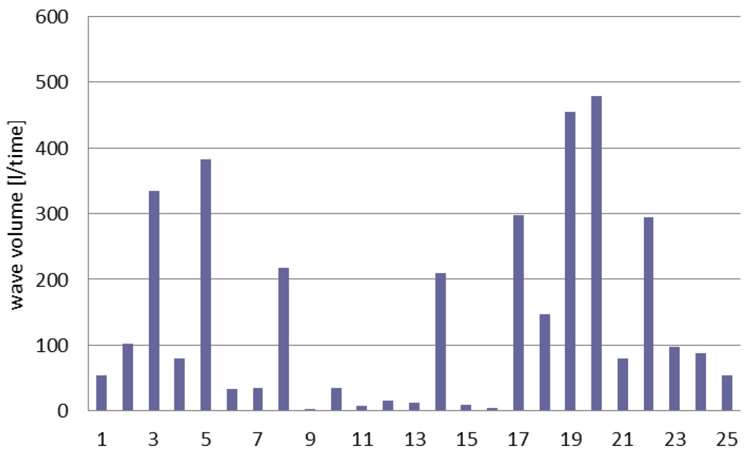

Table 6-1: Wave overtopping discharge in different wave trains
(dx = 0.5 m; wave properties are total one, not incident) ~100 waves:20 min

Wave train*	Conditions	Dx	H_{m0} at 071	$T_{m-1,0}$ at 071	Overtopping	Number of overtopping
[-]	[-]	[m]	[m]	[s]	[l/m/s]	[times/20 min]
-	**Measurement**	-	**2.54**	**14.7**	**1.4**	**25**
Wt0	SWASH 1D	0.5	2.74	13.2	1.6	5
Wt1	SWASH 1D	0.5	2.61	13.9	2.7	9
Wt2	SWASH 1D	0.5	2.66	14.4	0.2	3
Wt3	SWASH 1D	0.5	2.73	14.3	5.2	9
Wt4	SWASH 1D	0.5	2.70	13.3	3.3	9
Ave.	**SWASH 1D**	**0.5**	**2.69**	**13.8**	**2.6**	**7.0**
Err.			**+6%**	**-7%**	**Factor 1.9**	**Factor 0.3**
Wt0	SWASH 1D	0.1	2.74	13.4	0.7	5
Wt1	SWASH 1D	0.1	2.63	13.5	2.1	11
Wt2	SWASH 1D	0.1	2.60	14.3	0.1	3
Wt3	SWASH 1D	0.1	2.76	13.3	3.3	9
Wt4	SWASH 1D	0.1	2.66	13.0	1.4	9
Ave.	**SWASH 1D**	**0.1**	**2.68**	**13.5**	**1.5**	**7.4**
Err.			**+6%**	**-8%**	**Factor 1.1**	**Factor 0.3**

*Seed number of Wt0 is default, Wt1 is 11111111, Wt2 is 22222222, Wt3 is 33333333 and Wt4 is 44444444.

Table 6-2: Wave overtopping discharge in each measurement from Petten

Case	**H_{m0}**	**q**	**N**
PT1	2.27	1.4	25
PT2	2.18	0	0
PT3	2.13	0.13	4
PT4	2.37	2.1	14

Table 6-3: Wave overtopping discharge in different wave trains
(dx = 0.5 m; wave properties are total one, not incident) 500 waves

Wave train*	Conditions	Dx	H_{m0} at 071	$T_{m-1,0}$ at 071	Overtopping	Number of overtopping
[-]	[-]	[m]	[m]	[s]	[l/m/s]	[times/100 min]
-	**Measurement**	**-**	**2.54**	**14.7**	**1.4**	**125**
Wt0	SWASH 1D	0.5	2.68	14.8	1.6	32
Wt1	SWASH 1D	0.5	2.65	13.9	1.7	37
Wt2	SWASH 1D	0.5	2.70	13.1	1.8	35
Wt3	SWASH 1D	0.5	2.65	14.2	1.7	40
Wt4	SWASH 1D	0.5	2.69	14.9	2.1	40
Ave.	**SWASH 1D**	**0.5**	**2.67**	**14.2**	**1.8**	**36.8**
Err.			**+5%**	**-4%**	**Factor 1.3**	**Factor 0.3**

*Seed number of Wt0 is default, Wt1 is 11111111, Wt2 is 22222222, Wt3 is 33333333 and Wt4 is 44444444.

6.1.3 EurOtop (2007) overtopping calculation based on SWASH 2D calculation

EurOtop (2007) is used to estimate wave overtopping discharge in the case of Petten. For the input of EurOtop, incident wave information is necessary. However the incident wave information was not measured in the field. In this study, SWASH 2D calculation result (stated above) is used for the input of the wave overtopping calculation in Petten by EurOtop. Equations 5.9 have been applied to this calculation.

The result is shown in Table 6-4. The overtopping calculation by EurOtop also gives reasonable overtopping discharge. Actually Petten configuration is still 'deep water' condition since the water depth at the toe is almost 5 m (+2.82 m TAW water level - 2m TAW at the toe: in total 5 m). Therefore the equation applied here is Equation 5.9 in EurOtop. See Altomare *et al.* (2016) for the detailed instruction for the overtopping calculation.

Table 6-4: Wave overtopping calculation by EurOtop (Eq 5.9)

Conditions	Incident H_{m0} at 071	Incident $T_{m-1,0}$ at 071	Xsi number at 071	Number of overtopping	Overtopping
[-]	[m]	[m]	[-]	[times/20 min]	[l/m/s]
EurOtop (2007)	2.13	9.7	1.5	29	0.8
In-situ measurement	-	-	-	25	1.4

6.1.4 Conclusion

Both SWASH model and EurOtop give reasonable overtopping discharge for the Petten case (short wave dominant case).

However the computation has been conducted using only one example. This kind of exercises should be accumulated to be able to judge the quality of the calculation.

Note that the Petten case is not a 'shallow foreshore' case since the breaker parameter is 4.2.

6.2 Wenduine case

In this section, wave overtopping performance in SWASH is checked by Wenduine physical model test. WEN_004 has been used since this case does not have storm return walls and the EurOtop methodology can be applied in this case.

6.2.1 Model settings

The test conditions are defined below.

- Profile: Wenduine (simplified model)
  - Slope: 1/35 (foreshore) and 1/2 (dike)
  - Toe level: +6.7 m TAW
  - Case 004: without sea wall but there is a berm (~90 cm in the scale model, see Figure 6-3)
- Hydraulic boundary condition: 1000 year storm
  - Water level: +6.84 m TAW
  - Wave height (H_{m0}): 4.75 m
  - Wave period (T_p): 11.7 s

Figure 6-3: Wenduine physical model

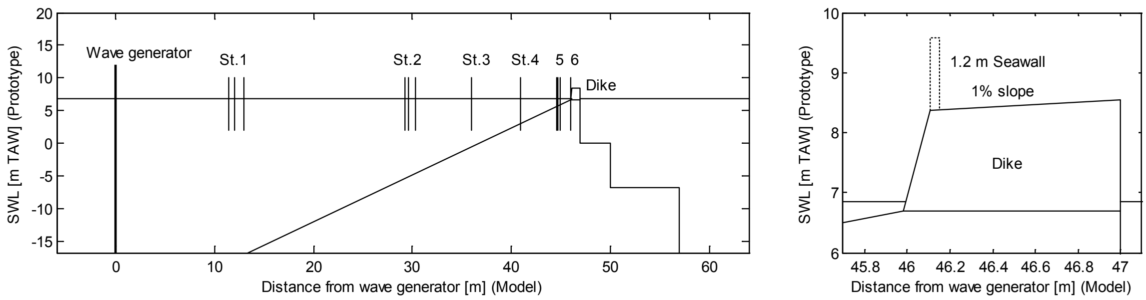

Numerical simulations were carried out with SWASH (version 2.00 from swash.sf.net). The physical model layouts as in Figure 6-3 were reproduced in the SWASH numerical domain. The total length of the numerical model domain from the upstream boundary to the end of the sea dike was set to the same dimensions as the physical model. In some cases, the basins behind the dike crest were extended in order to provide sufficient volume to collect water overtopping the sea dike. The grid size in the x-direction was set as 0.02 m for all cases. The model was run with one layer in the vertical direction since the kd value was less than 1 in all cases, indicating that the estimated phase velocity error is insignificant (where k is the wave number and d the water depth).

The wave properties described above (Hydraulic boundary condition: 1000 year storm) were prescribed at the wave boundary in the numerical model simulations with a weakly reflective boundary condition. 1^{st} order and 2^{nd} order wave generations were tested. A Sommerfeld radiation condition was applied at the downstream end of the numerical domain in order to minimize the effect of the reflection. A still water level was applied as the initial condition for all numerical models tests.

The time duration of the numerical simulations was the same as used in the physical model experiments, approximately 40 min in the model scale to generate 1000 waves. The numerical time step is automatically changed during SWASH calculations to satisfy the Courant–Friedrichs–Lewy (CFL) condition. The Manning's n roughness parameter has an influence on mean wave overtopping discharge, particularly when there is long run-up zone and long berm. A Manning coefficient of n=0.000 and 0.012 s/m$^{1/3}$ were tested.

In order to show the basic performance of the SWASH one-layer model, the breaking parameters (see details in Smit *et al.*, 2013) are fixed as default values (i.e. no tuning for wave transformation and overtopping by choosing alternative wave breaking parameters). Note that SWASH accounts for wave energy dissipation even without the breaking parameters due to inherent nature of the equation (for further explanation in SWASH user manual, (The SWASH team, 2016).

The non-hydrostatic pressure term was applied with a Keller-box scheme, which has significant influence on wave transformation. Explicit time integration was used with a time step restriction set to a maximum Courant number of 0.5 as recommended in SWASH user manual (The SWASH team, 2016).

6.2.2 Wave overtopping calculation

Table 6-5 shows the wave overtopping results from the physical model and the SWASH 1D model. Case 1 is physical model test conducted in FHR (Case WEN_004), and Case 2-7 are SWASH 1D validation and sensitivity tests (changing 1st order/2nd order, bottom friction, dx). Case2 is a validation case against Case 1 (physical model). The wave generation of the paddle in the wave flume in FHR is based on the 1st order wave generation, therefore this case is most suitable to check the performance of SWASH 1D. Case 3 is without berm: removed the berm and raised the crest level to the same level as in the crest level of the berm.

Physical model (Case 1) and most of the SWASH calculation cases (Case 2-7) have a dike inside the model: in those cases incident wave height is difficult to get since the non-linearity is too high to apply Mansard and Funke (1980) method to get incident wave height. Therefore the dike is removed when it is necessary to get incident wave height (Case 8-10 in Table 6-5).

Table 6-5: Wave overtopping calculations (1D): Test Case WEN_004

Case	Model	Bottom friction	Wave gen	dx	Overtopping calculation
1	**Physical model**	**-**	**1st order**	**-**	**72 l/s/m***
2	SWASH 1st order	0.012	1st order	0.5 m	55 l/s/m*
3	SWASH 1st order without berm	0.012	1st order	0.5 m	74 l/s/m*
4	SWASH no friction	0.000	2nd order	0.5 m	24 l/s/m*
5	SWASH standard case	0.012	2nd order	0.5 m	27 l/s/m*
6	SWASH coarse grid (1m)	0.012	2nd order	1.0 m	19 l/s/m*
7	SWASH coarse grid (2m)	0.012	2nd order	2.0 m	17 l/s/m*

*calculated by SWASH 1D overtopping calculation.

6.2.3 Influence of bottom friction

Influence of bottom friction is further investigated here using other Wenduine physical model test cases (Case 042, 027, 041, 017, 018, 124, 125, 126, 026, 024, op top of 004). Two different bottom friction parameters have been tested (Manning; n=0.000, no friction and n=0.012, smooth wood) in SWASH 1D overtopping calculation. Note that the calculation is conducted using SWASH version 3.14 here (therefore the result is slightly different from the one in the last section).

Figure 6-4 shows the computed overtopping discharge using SWASH with different n values, and measured overtopping discharge in the physical model test.

The result shows that the overtopping discharge calculated using n=0.000 represents the physical model test results better.

Figure 6-4: SWASH 1D overtopping calculation using n=0.000 and n=0.012

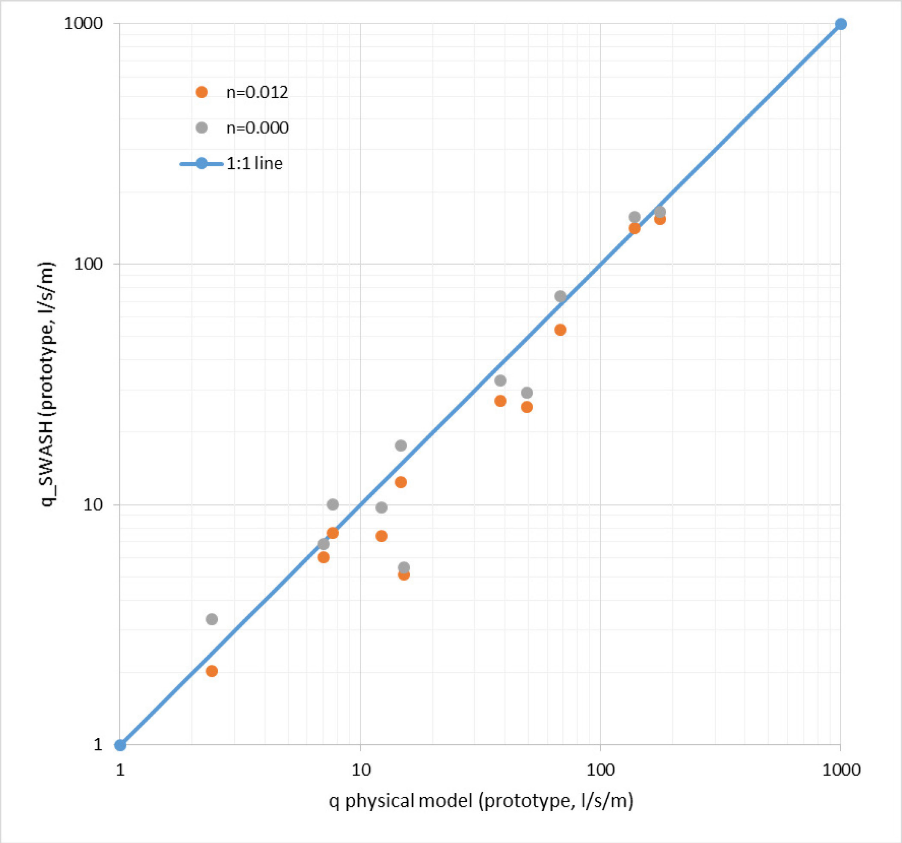

Key conclusions from these calculations are as follows.

- SWASH 1D 1st order calculation gives a reasonable estimation (55 l/s/m).
- Berm effect (1% slope) is ~35% (74/55=135%)
- Bottom friction does not give so much change in such a high overtopping discharge cases. However details can be investigated for small overtopping discharge cases. Note that bottom friction is activated from the paddle position, so that incident wave height might be slightly over- or underestimated in each case. As a consequence, the estimated value q cannot evaluate the influence of the bottom friction purely (e.g. in some case no bottom friction gives less q).
- 2nd order wave generation gives a smaller overtopping discharge compared to 1st order.
- The grid resolution has an impact on the wave overtopping discharge (27->17 l/s/m).
- From these calculations it can be concluded that the SWASH 1D overtopping calculation gives realistic overtopping discharges, although with a tendency to underestimate the discharge
- SWASH represents overtopping discharge phenomenon better using n=0.000 (no friction).

6.3 Physical model of Van Doorslaer & De Rouck (2010)

6.3.1 Physical Model Setup

The laboratory flume tests of Van Doorslaer & De Rouck (2010) are considered to further validate the SWASH model for wave overtopping of a sea dike. These tests feature a smooth, impermeable sea dike, with a deep water condition at the toe of the structure; refer to Figure 6-5.

The 2D physical model experiments were performed at scale 1:20 in the wave flume at Ghent University. This flume measures 30 m long, 1.0 m wide and 1.2 m high. Waves are generated using a piston type wave paddle with active wave absorption. For physical model tests a JONSWAP wave spectrum with gamma =3.3 was generated with the wave paddle and the total number of waves generated was 1000.

Wave height measurements were obtained with eight resistive- type wave gauges installed at the locations summarized in Figure 6-5. Mean wave overtopping discharge was evaluated by collection of overtopping water in a box situated behind the dike, and dividing the total volume collected by the test duration. Individual wave overtopping volumes were not measured in these experiments.

Figure 6-5: Physical and numerical model domains (prototype scale) for Case 2

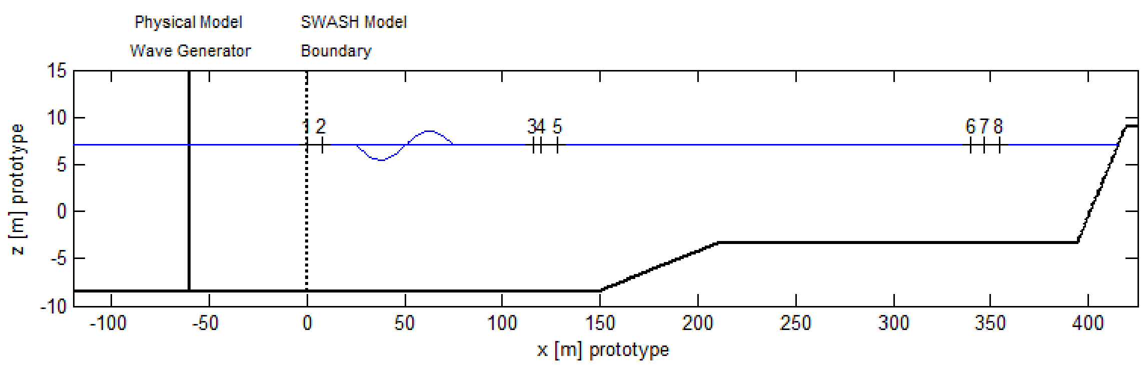

6.3.2 Numerical Model Setup

The physical model topography, as shown in Figure 6-5, was reproduced in the numerical domain using SWASH. The upstream boundary of the numerical model coincides with wave gauge No. 1, and the total length of the model from the upstream boundary to the end of the crest of the sea dike was 420 m. An additional basin of 480 m in length was added downstream of the sea dike in order to provide sufficient volume to collect water overtopping the sea dike. The total numerical domain was therefore 900 m, with a mesh size in the x-direction of 0.5 m. The model was run with one layer in the vertical direction.

A JONSWAP wave energy spectrum, with γ = 3.3, was applied as a weakly reflective boundary condition in the numerical simulations. A Sommerfield radiation condition was applied at the end of the numerical domain in order to minimize the effect of the reflection. The still water level was applied as the initial condition for all numerical models tests.

The duration of the numerical simulation was the same as used in the physical model experiments, approximately 3 hours in prototype scale in order to generate at least 1000 waves, with a numerical time step of 0.02 s. A Manning roughness value n=0.01 was used for all model tests.

Table 6-6: Overtopping test parameters

TEST NAME	SWL m TAW	H_{m0} m	T_p s	$T_{m-1,0}$ s	DIKE SLOPE cot()	DIKE TOE LEVEL m TAW	DIKE CREST LEVEL m TAW	WALL CREST LEVEL m TAW	WALL LOCATION
GEN_001	7	2.5	12	11	2	-3.4	9	NA	NA
GEN_002	7	2	12	11	2	-3.4	9	NA	NA
GEN_003	7	1.5	12	11	2	-3.4	9	NA	NA
GEN_004	7	2.5	10	9	2	-3.4	9	NA	NA
GEN_005	7	2	10	9	2	-3.4	9	NA	NA
GEN_006	7	1.5	10	9	2	-3.4	9	NA	NA
GEN_007	6	2.5	12	11	2	-3.4	9	NA	NA
GEN_008	6	2	12	11	2	-3.4	9	NA	NA
GEN_009	6	1.5	12	11	2	-3.4	9	NA	NA
GEN_010	6	2.5	10	9	2	-3.4	9	NA	NA
GEN_011	6	2	10	9	2	-3.4	9	NA	NA
GEN_012	6	1.5	10	9	2	-3.4	9	NA	NA

6.3.3 Wave Propagation

The total energy spectra evaluated with the SWASH numerical model at wave gauge No. 2, 4 and 7 are given in Figure 11 for test GEN_001. The spectra show that the JONSWAP spectrum show remains largely unchanged from offshore to onshore due to the deep water condition at the dike. This is also reflected in the propagation of wave height (H_{m0}) and period ($T_{m-1,0}$, T_p) and wave setup which are plotted in Figure 12. These data are based on the entire wave spectrum, thus including both incident and reflected waves.

Figure 6-6: Energy density spectra computed with the numerical model (black line) and the JONSWAP spectrum with H_{m0} = 2.5; T_p = 12 s and γ = 3.3 (red line) at different stations for test case GEN_001

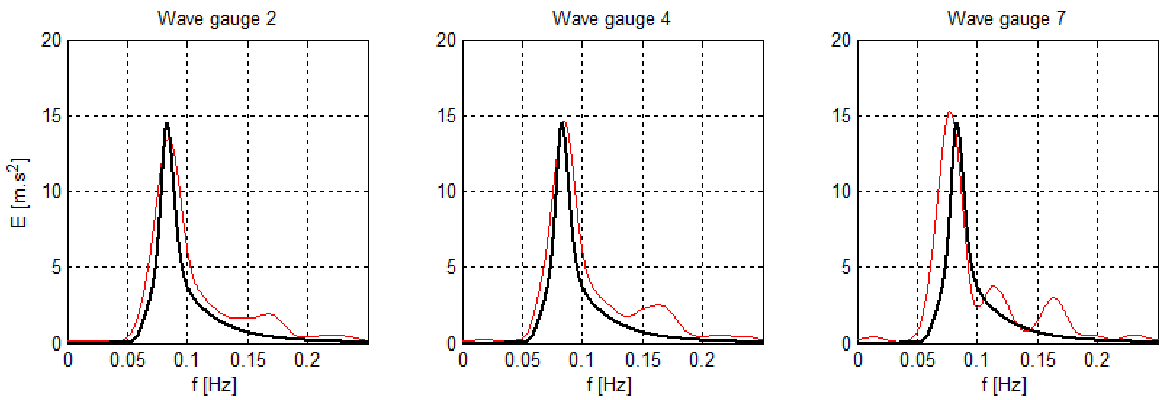

Figure 6-7: (a) Significant wave height, H_{m0} (b) wave period, $T_{m-1,0}$ (c) wave setup and (d) wave period, T_p computed by numerical model for test case GEN_001

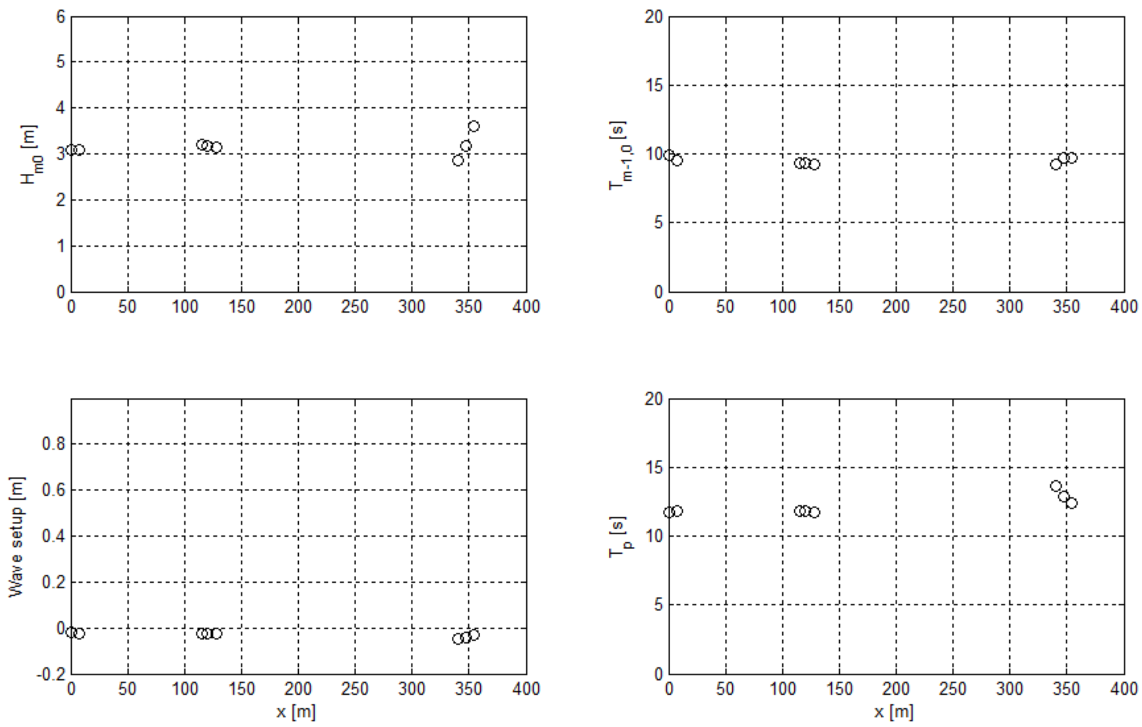

6.3.4 Mean Wave Overtopping

The mean wave overtopping discharge in the numerical model was evaluated using the same method described in section 6.2.1. Table 4 lists mean wave overtopping discharge measured from the numerical model for each test case.

Incident wave height (Hm0) and period (Tm-1,0) at the toe of the dike are also listed in Table 2, and have been calculated by applying a reflection analysis using measurements from wave gauges No. 6, 7 and 8 , according to the method of Mansard and Funke (1980).

The EurOtop (2007) empirical equation for wave overtopping with non-braking waves (ξm-1,0 < 5) is most suitable for this experimental setup, and is reproduced as Equation 5, where Rc* and q* are defined in Equations 6 and 7. Freeboard, Rc, is measured from the crest of the dike or wave wall to the still water level. The overtopping reduction factor, γ, has been set equal to 1.0 for this study. Figure 13 plots the mean wave overtopping measured in the numerical model in non-dimensional form, based on the EurOtop (2007) empirical equation for non-breaking waves. This figure indicates that all measured data fits within the 95% confidence intervals given by this equation.

The derived line of best fit from physical model experiments is also plotted in Figure 13. This shows that the SWASH model slightly underestimates mean wave overtopping discharge relative to the physical model line of best fit, this may also be due to the reasons outlined in section 6.2.2. However the numerical model shows good agreement with the EurOtop (2007) equation for non-breaking waves.

$$q^* = 0.2.\exp\left(-2.6.R_c{}^*\right) \quad (5$$

$$q^* = \frac{q}{\sqrt{g \cdot H_{m0}{}^3}} \quad (6$$

$$R_c{}^* = \left(\frac{R_c}{\gamma \cdot H_{m0}}\right) \quad (7$$

Table 6-7: Measured incident wave H_{m0} and $T_{m-1,0}$ and mean overtopping discharge ($\overline{q}$)

TEST NAME	SWASH Model (computed)		
	H_{m0} m	$T_{m-1,0}$ s	$\overline{q}$ l/s/m
GEN_001	2.55	12.32	274
GEN_002	2.07	11.90	138
GEN_003	1.56	11.46	45.6
GEN_004	2.51	11.53	247
GEN_005	2.03	10.86	123
GEN_006	1.54	10.12	38.8
GEN_007	2.57	11.99	125
GEN_008	2.08	11.67	51.1
GEN_009	1.58	11.29	10.6
GEN_010	2.53	11.58	93.0
GEN_011	2.04	10.82	32.9
GEN_012	1.55	10.05	4.65

Figure 6-8: Non-dimensional computed (crosses) mean wave overtopping discharge plotted against EurOtop (2007) equation (thick line) for shallow foreshores

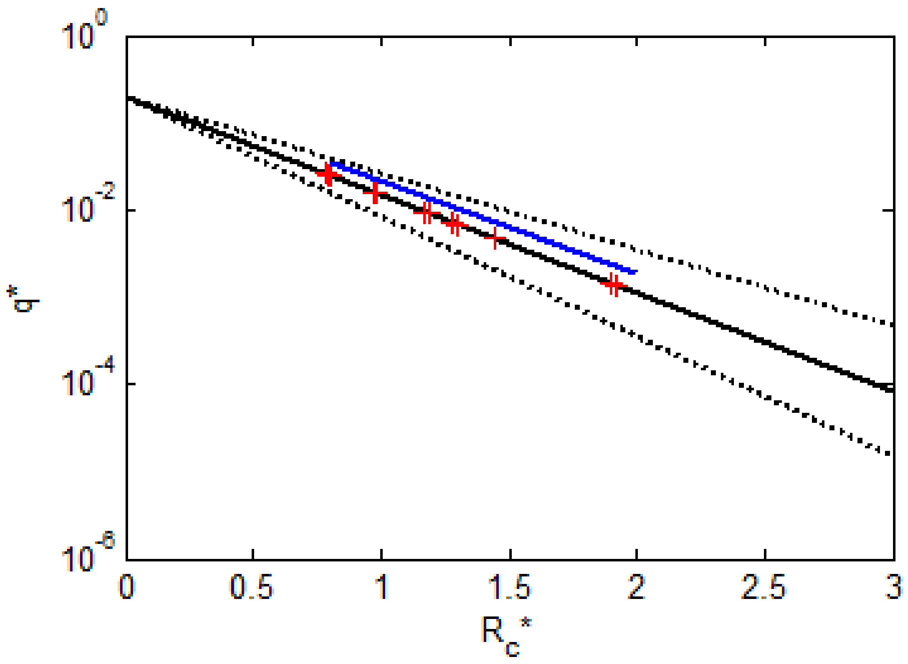

Dotted lines are 5% upper and lower exceedence limits and blue line is UGent physical model line of best fit

6.4 Conclusion

SWASH 1D wave overtopping calculation for the Petten case (short wave dominant case; in-situ measurement), Wenduine case (long wave dominant case; physical model), UGent case (short wave dominant case; physical model) has been tested in this chapter.

The Petten case proved that the SWASH 1D wave overtopping calculation method in combination with SWASH 2D calculation for wave transformation works well.

Wenduine (long wave dominant case) and UGent case (short wave dominant case) proved that the SWASH 1D wave overtopping calculation method works well for both short and long waves in a 1D flume case.

7 Case study for wave overtopping calculation

7.1 Wenduine case study

In this section, the proposed methodology to be used in the 'Safety Assessment 2015' is compared to the last methodology used in the 'Safety Assessment 2007'.

Table 7-1 shows the comparison between a SWASH 1D overtopping calculation in combination with SWASH 2D, overtopping calculation based on Altomare *et al.* (2016) in combination with SWASH 2D and the overtopping calculation in the 'Safety Assessment 2007'.

SWASH 1D overtopping calculation in combination with SWASH 2D gives a higher value than the overtopping calculation in the 'Safety Assessment 2007'. However the value is not so different even though the methodology has been totally changed. Altomare *et al.* (2016) gives higher value than SWASH 1D overtopping calculation in combination with SWASH 2D case since Altomare *et al.* (2016) value is deterministic value, which leads to about 2 times higher value than probabilistic one.

Table 7-1: Wave overtopping estimation in Wenduine (WEN_004: crest level of 8.56 m TAW at the end of the dike)

Conditions	Incident H_{m0} at toe	Incident $T_{m-1,0}$ at toe	Set-up	Overtopping
[-]	[m]	[s]	[m]	[l/m/s]
SWASH 2D + SWASH 1D	0.90 (+3%)	49.9 (+8%)	**+7.10 m TAW** + 0.20 (-1 cm from +6.87 m TAW + 0.44)	9.3*
SWASH 2D + Altomare et al. (2016)	0.90 (+3%)	49.9 (+8%)	**+7.10 m TAW** + 0.20 (-1 cm from +6.87 m TAW + 0.44)	17.5**
SWAN 1D at 5Hs & Wind + EurOtop (2007)	0.90 (at x=1125m)	8.5 (at x=1125m)		5.1***

*calculated by wave overtopping calculation by SWASH 1D.

**calculated based on Altomare *et al.* (2016). Crest level is +8.56 m TAW but the berm is ignored.

***calculated from EurOtop (2007) Eq 5.10. Crest level is +8.56 m TAW but the berm is ignored.

7.2 Case study - special cross sections & Koksijde

Wave overtopping is calculated for the case with special cross sections and the Koksijde case (Table 7-2).

Incident wave properties are calculated by SWASH 2D, for a model without dike. Overtopping is calculated in Altomare *et al.* (2016) and SWASH 1D.

SWASH 1D wave overtopping calculation gives different results for long berm case and short berm case since the berm length is different. While Altomare *et al.* (2016) does not give different result for both cases since the berm effect was not taken into account.

The results show that the SWASH 1D direct wave overtopping calculation give very comparable value to Altomare *et al.* (2016).

Table 7-2: Wave overtopping estimation in special cross section case and Koksijde case

Conditions [-]	Foreshore slope [tan]	Toe [m TAW]	Dike slope (lower) [tan]	Level between slopes [m TAW]	Dike slope (upper) [tan]	Crest [m TAW]	Incident H_{m0} at toe [m]	Incident $T_{m-1,0}$ at toe [s]	Overtopping Methodology book [l/m/s]	SWASH 1D overtopping cal [l/m/s]
Special cross-section case: Small sand berm	43	6.5	10.0	7.3	3.0	9.3	1.15	34.2	3.3	7.0
Special cross-section case: Long berm	43	6.5	2.4	9.0	3.3	9.8	1.14	35.5	1.0	0.0
Special cross-section case: Short berm	43	6.5	2.4	9.0	3.3	9.8	1.14	35.5	1.0	0.9
Koksijde case	70	5.0	2.8	N.A.	N.A.	10.2	1.50	20.2	2.5	4.9

8 Conclusions

8.1 Wave transformation

The main conclusions for the wave transformation models are shown as follows.

- SWASH, Mike21BW and SWAN have been tested to select the methodology for wave transformation in the ‘Safety Assessment 2015’. Each model has pros and cons, but SWASH 2D gives the most reasonable result: the long waves were reproduced very well while computational cost is acceptable.
- By means of validation, 4 cases from Petten and 3 cases from Oostende Noodstrand were applied to the SWASH 2D. Wave energy is slightly overestimated in some points but most of the results show a good agreement to the in-situ measurement data. Since this is the comparison between numerical model and field measurement, some difference can be expected. The differences are due to the difference of data set and simulation settings (e.g. bathymetry data are not exactly the same; wind information is not used in the numerical simulation; tidal/local current are not used in the numerical simulation; time series of waves are unknown, etc).
- The 2D SWASH model gives a good estimation for wave transformation from -5 m TAW to the toe of the dike, therefore it is chosen as a wave transformation model for the ‘Safety Assessment 2015’.

8.2 Wave overtopping

The main conclusions for the wave overtopping model used by SWASH 1D are summarized hereafter:

- SWASH 1D overtopping calculation gives reasonable overtopping discharges both for short wave dominant case and long wave dominant case. A better prediction of the overtopping discharge is obtained in cases dominated by long waves.
- There’s some uncertainty involved in the simulation of the number of wave overtopping events for SWASH 1D wave overtopping calculation.
- Bottom friction n=0.000 gives better results for Wenduine physical model test. Therefore no bottom friction is proposed for the ‘Safety Assessment 2015’.
- The SWASH 1D overtopping calculation is chosen as a wave overtopping model for the ‘Safety Assessment 2015’ since it is applicable for some complex cases (berm and vertical wall) where the empirical equation from Altomare *et al.* (2016) is not applicable, and this with a reasonable computation cost.

8.3 Differences in outcomes from the ‘Safety Assessment 2007’ and ‘2015’

The differences in several aspects of the methodology between the ‘Safety Assessment 2007’ and ‘2015’ are listed below with ‘+’ and ‘–‘ is added at each change: + indicates an increase of overtopping discharge and ‘-‘ shows a decrease of overtopping. (Note that the + and – are just an estimation).

- Bathymetry is updated (+-)
- Hydraulic boundary condition at -5 m TAW is updated (+-)
- 'Wave boundary condition at toe of dike' is moved to the toe of the dike location from $5H_{m0}$ distance from the dike about 25 m offshore (-)
- Low frequency waves are included by the time domain computation by the SWASH model (++)

For the same geometry, the overtopping discharge stays almost in the same range taking into account those + and - notations.

Finally all the detailed methodologies related to wave transformation and wave overtopping using SWASH for 'Safety Assessment 2015' are summarized in Suzuki *et al.* (2016).

9 References

Altomare, C.; Suzuki, T.; Chen, X.; Verwaest, T.; Kortenhaus, A. (2016). Wave overtopping of sea dikes with very shallow foreshores. *Coast. Eng. 116*: 236–257. doi:10.1016/j.coastaleng.2016.07.002

Altomare, C.; Suzuki, T.; Spiesschaert, T.; Verwaest, T.; Mostaert, F. (2014). SUSCOD Pilot 1: Wenduine wave overtopping scale model: final report. *WL Rapporten*, 00_025. Flanders Hydraulics Research: Antwerp

Barthel, V.; Mansard, E.P.D.; Sand, S.E.; Vis, F.C. (1983). Group bounded long waves in physical models. *Ocean Eng. 10*(*4*): 261–294. doi:10.1016/0029-8018(83)90012-4

Battjes, J. a; Groenendijk, H.W. (2000). Wave height distributions on shallow foreshores. *Coast. Eng. 40*(*3*): 161–182. doi:10.1016/S0378-3839(00)00007-7

Booij, N.; Ris, R.C.; Holthuijsen, L.H. (1999). A third-generation wave model for coastal regions 1 . Model description and validation *104*: 7649–7666

Danish Hydraulic Institute. (2015). Mike 21 Wave Modelling

De Roo, S.; Trouw, K.; Ruiz Parrado, I.; Suzuki, T.; Verwaest, T.; Mostaert, F. (2016). Het Hydraulisch randvoorwaardenboek (2014). *WL Rapporten*, 14_014. Waterbouwkundig Laboratorium/Fides Engineering: Antwerpen

Delft Hydraulics and Alkyon. (2003). Reliability of SWAN at the Petten Sea Defence

Den Heijer, F. (1998). Golfoverslag en krachten op verticale waterkeringsconstructies

Gruwez, V.; Bolle, A.; Suzuki, T.; Verwaest, T.; Mostaert, F. (2012). Numerieke modellering van het extreem golfklimaat in de Belgische havens: deel 2: haven van Zeebrugge. *WL Rapporten*, 769_03. Waterbouwkundig Laboratorium/IMDC: Antwerpen

Guza, R.T.; Feddersen, F. (2012). Effect of wave frequency and directional spread on shoreline runup. *Geophys. Res. Lett. 39*(*11*): n/a-n/a. doi:10.1029/2012GL051959

Herbers, T.H.C.; Elgar, S.; Guza, R.T. (1995). Infragravity-frequency (0.005–0.05 Hz) motions on the shelf. Part I: forced waves. *J. Phys. Ocean. 24*(*5*): 917–927

IMDC. (2008). Geïntegreerd Kustveiligheidsplan

Ottesen Hansen, N.E.; Sand, S.E.; Lundgren, H.; Sorensen, T.; Gravesen, H. (1979). CORRECT REPRODUCTION OF GROUP-INDUCED LONG WAVES, ***in***: (1979). *ICCE 1980*. ISBN 9781617798214. pp. 1–15. doi:10.1007/978-1-61779-821-4

Pullen, T.; Allsop, N.W.H.; Kortenhaus, A.; Schüttrumpf, H.; Troch, P.; Van der Meer, J.W. (2007). EurOtop. ISBN 9783804210646. Available at: www.overtopping-manual.com

Roelvink, D.; Reniers, A.; van Dongeren, A.; van Thiel de Vries, J.; McCall, R.; Lescinski, J. (2009). Modelling storm impacts on beaches, dunes and barrier islands. *Coast. Eng. 56*(*11–12*): 1133–1152. doi:10.1016/j.coastaleng.2009.08.006

Smit, P.; Zijlema, M.; Stelling, G. (2013). Depth-induced wave breaking in a non-hydrostatic, near-shore wave model. *Coast. Eng. 76*: 1–16. doi:10.1016/j.coastaleng.2013.01.008

Suzuki, T.; Altomare, C.; Verwaest, T.; Trouw, K.; Zijlema, M.; Fluid, E.; Section, M. (2014). Two-dimensional wave overtopping calculation over a dike in shallow foreshore by swash, ***in***: (2014). *International Conference on Coastal Engineering*

Suzuki, T.; De Roo, S.; Altomare, C.; Zhao, G.; Kolokythas, G.K.; Willems, M.; Verwaest, T.; Mostaert, F.

(2016). Toetsing kustveiligheid-2015 - Methodologie: toetsingsmethodologie voor dijken en duinen. Versie 10. *WL Rapporten*, 14_014. Waterbouwkundig Laboratorium: Antwerpen

Suzuki, T.; Gruwez, V.; Bolle, A.; Verwaest, T.; Mostaert, F. (2012). Numerical modelling of the extreme wave climate in the Belgian harbours: part 3. Marina of Blankenberge. *WL Rapporten*, 769_03. Waterbouwkundig Laboratorium/IMDC: Antwerp

Suzuki, T.; Verwaest, T.; Hassan, W.; Veale, W.; Reyns, J.; Trouw, K.; Troch, P.; Zijlema, M. (2011). The applicability of SWASH model for wave transformation and wave overtopping: A case study for the Flemish coast, ***in***: (2011). *Proceedings of the 5th International Conference on Advanced COmputational Methods in ENgineering (ACOMEN 2011), 14-17 November 2011, Liège, Belgium*. Université Catholique de Louvain/Université de Liège/Universiteit Gent. ISBN 978-2-9601143-1-7. pp. [1-11]

Suzuki, T.; Verwaest, T.; Veale, W.; Trouw, K.; Zijlema, M. (2012). A Numerical Study on the Effect of Beach Nourishment on Wave, ***in***: (2012). *ICCE 2012*. pp. 1–13

Suzuki, T.; De Roo, S.; Altomare, C.; Peeters, P. ; Mostaert, F. (2017). Methodology for safety assessment 2015 - Updated methodologies from the report ver 6.0 to ver 10.0 (under review)

TAW. (2002). Wave Run-up and Wave Overtopping at Dikes Wave Run-up and Wave Overtopping at Dikes

The SWASH team. (2016). SWASH USER MANUAL: SWASH version 3.14A

Van Doorslaer, K.; De Rouck, J. (2010). REDUCTION OF WAVE OVERTOPPING ON A SMOOTH DIKE BY MEANS OF A PARAPET, ***in***: (2010). *International Conference on Coastal Engineering (ICCE 2010), Shanghai, China.* pp. 1–15

Van Doorslaer, K.; Rouck, J. De; Audenaert, S.; Duquet, V. (2015). Crest modi fi cations to reduce wave overtopping of non-breaking waves over a smooth dike slope. *Coast. Eng. 101*: 69–88. doi:10.1016/j.coastaleng.2015.02.004

Vanneste, D.; Altomare, C.; Suzuki, T.; Troch, P.; Verwaest, T. (2014). Comparison of numerical models for wave overtopping and impact on a sea wall, ***in***: (2014). *Proceedings of 34th Conference on Coastal Engineering, Seoul, Korea, 2014*. *Coastal Engineering Proceedings*, 34. Coastal Engineering Research Council. ISBN 978-0-9896611-2-6. pp. [1-14]

Vledder, G. van; Ruessink, G.; Rijnsdorp, D. (2013). Individual wave height distributions in the coastal zone: Measurements and simulations and the effect of directional spreading. *Coast. Dyn.* 1799–1810. doi:10.1128/JCM.00586-13

Wenneker, I.; Spelt, B.; Peters, H.; Ronde, J. De. (2016). Overview of 20 years of fi eld measurements in the coastal zone and at the Petten sea dike in the Netherlands. *Coast. Eng. 109*: 96–113. doi:10.1016/j.coastaleng.2015.12.009

Zijlema, M.; Stelling, G.; Smit, P. (2011). SWASH: An operational public domain code for simulating wave fields and rapidly varied flows in coastal waters. *Coast. Eng. 58*(*10*): 992–1012. doi:10.1016/j.coastaleng.2011.05.015

Appendix A: directional spreading

There are several models to express directional spreading distribution. These expressions are introduced here.

Cos model

This model is used in SWAN. Directional spreading (DSPR, hear after) is specified by the value of m.

$$D(\theta) = A_1 \cos^m \theta$$

The m value (MS in the table) is translated into DSPR by the table below. See actual spreading example in the figure below.

Table : Directional distribution

MS	DSPR (in ^{o})
1.	37.5
2.	31.5
3.	27.6
4.	24.9
5.	22.9
6.	21.2
7.	19.9
8.	18.8
9.	17.9
10.	17.1
15.	14.2
20.	12.4
30.	10.2
40.	8.9
50.	8.0
60.	7.3
70.	6.8
80.	6.4
90.	6.0
100.	5.7
200.	4.0
400.	2.9
800.	2.0

Cos2 model

This model is used in SWAN and SWASH. DSPR is specified by the value of s.

$$D(\theta) = A_2 \cos^{2s}\left(\frac{1}{2}\theta\right)$$

The s value is translated into DSPR (σ_ϑ) by equation below.

$$\sigma_\theta = \sqrt{\frac{2}{s+1}}$$

Comparison of cos model and cos2 model

Both model give similar distribution for DSPR=31.5 and DSPR=14.2 degree.

Figure : Comparison of the shape of directional spreading distribution

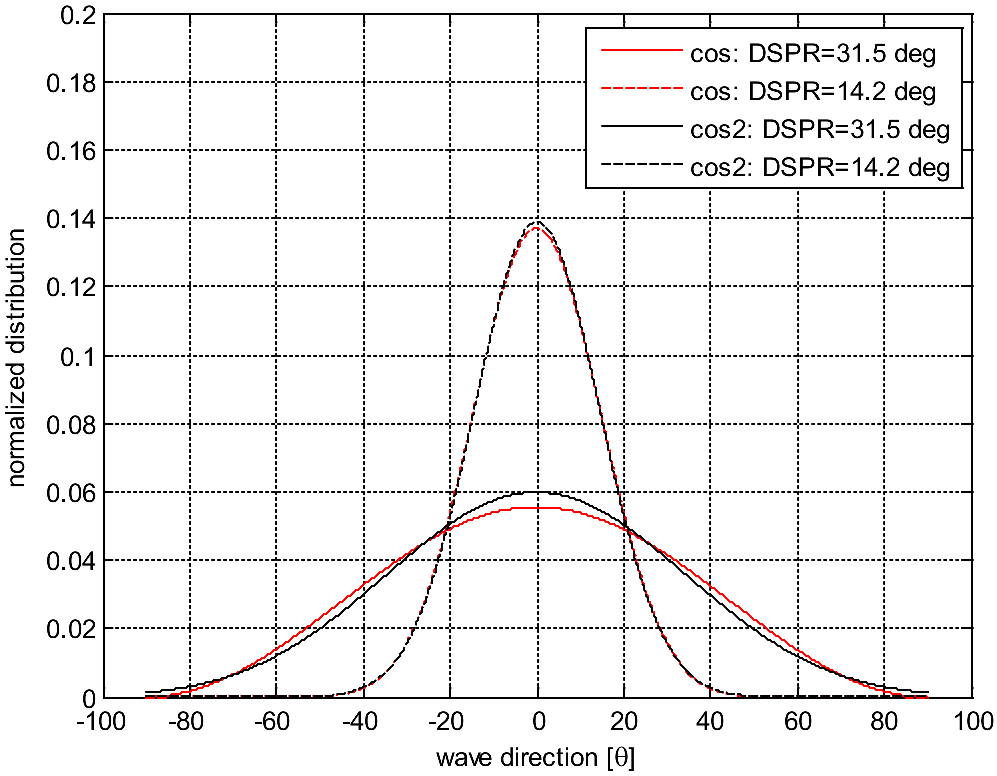

DEPARTMENT **MOBILITY & PUBLIC WORKS**
Flanders hydraulics Research

Berchemlei 115, 2140 Antwerp
T +32 (0)3 224 60 35
F +32 (0)3 224 60 36
waterbouwkundiglabo@vlaanderen.be
www.flandershydraulicsresearch.be